MODIFICATION OF THE HYDRATION PRODUCTS OF HYDRATED CEMENT PASTE BY FLY ASH, *β*-CYCLODEXTRIN AND FLY ASH-*β*-CYCLODEXTRIN COMPOSITE

Ikotun B.D. [1*], Mishra S. [2], Fanourakis G.C. [3]

(1) Department of Civil and Chemical Engineering, College of Science, Engineering and Technology, University of South Africa, Johannesburg 1710, South Africa.
(2) Nanotechnology and Water Sustainability Unit, College of Science, Engineering and Technology, University of South Africa, Florida Campus, Johannesburg, South Africa.
(3) Department of Civil Engineering Technology, Faculty of Engineering, University of Johannesburg, South Africa.

ABSTRACT

Studies on the modification of the hydration products of fly ash (FA), *β*-cyclodextrin (*β*-CD) and fly ash-*β*-cyclodextrin (FA-*β*-CD) composite cement paste samples as hydration progressed were done using X-ray diffraction (XRD) analysis, scanning electron microscopy **(**SEM) and Fourier transform infrared spectroscopy (FT-IR). The interaction between FA and *β*-CD has been shown by the authors in the previous article to have formed a composite that might improve hydration and pozzolanic reaction of cement and pozzolanic cement paste. This paper investigates the effect of FA, *β*-CD and FA-*β*-CD composite on the hydration and pozzolanic reactions. It was evident from all the analyses that *β*-CD improved the hydration reaction from the 7 day hydration period, while improvement on pozzolanic reaction was revealed from the 28 day hydration period. The study contributed to the knowledge of FA performance as a composite with cyclodextrin and promoted the continued inclusion of FA in concrete.

Keywords: Fly ash, Cyclodextrin, XRD, SEM, FT-IR, Hydration, Pozzolanic

1.0 INTRODUCTION

The process of setting and hardening of cement paste during the hydration reaction causes changes in the structure and microstructure as the process progresses. Observation of these changes helps to understand the behaviour of the final product. During the hydration period, cement compounds react to produce calcium hydroxide ($Ca(OH)_2$) and calcium silicate hydrate (C-S-H). C-S-H is responsible for strength development. During pozzolanic reaction, calcium hydroxide is consumed to form more C-S-H. In the process of hydration and pozzolanic reactions, changes in the different crystalline phases of tricalcium silicate (C_3S), dicalcium silicate (C_2S), tricalcium aluminate (C_3A), tetracalcium aluminoferrite (C_4AF), ettringite (calcium sulfoaluminate), calcium hydroxide ($Ca(OH)_2$), the amorphous phase of C-S-H and the morphology occur. The changes in these different phases help to understand the strength development from the mixing stage to the hardened stage. These changes are affected by different factors, such as the composition of cement, curing temperature, the solid/solution ratio and admixtures [1-3].

To understand the effect of fly ash (FA), *β*-cyclodextrin (*β*-CD) and fly ash- *β*-cyclodextrin (FA-*β*-CD) composite on concrete properties, the study of their effect on the hydration products formed during the hydration process of cement paste is important. FA dilutes the cement, such that less C-S-H from clinker is formed. It has been reported that in the presence of FA, hydration reaction slows down and leads to low early strength [4]. According to Aimin and Sarkar [5], the relatively slow gain of early strength due to FA, requires the need for an additional component to activate the hydrolysis ability of low calcium FA. Aimin and Sarkar [5] also added that the possibility of FA activation lies in the breaking down of its glass phases. A previous study by the authors [6] showed that the interaction of FA with cyclodextrin produced a composite that might affect the hydration and pozzolanic reactions

of cement. This article presents and discusses the effect of FA, β-CD and FA-β-CD composites on the modification of hydration products of cement paste samples during the hydration process. X-ray diffraction (XRD) analysis, scanning electron microscopy **(**SEM) and Fourier transform infrared spectroscopy (FT-IR) were employed for the investigation. Possible assignment of FT-IR bands as reported by Hughes et al [7] is shown in Table 1. This article does not limit the assignment of FT-IR bands to Table 1. The studies were monitored at different ages of hydration.

Table 1: Possible assignment of FT-IR absorption bands [7]

Mineral	Fundamentals			Overtones	O-H Stretch	O-H Bend
Sulfates	ν_1	ν_3	ν_4			
Gypsum	1005	1117	669, 604	2500–1900	3553, 3399	1686, 1618
Bassanite	1009	1152, 1117, 1098	660, 629, 600	2500–1900	3611, 3557	1618
Syngenite	1001	1192, 1130, 1113	658, 644, 604	2500–1900	3309	1678
Anhydrite	1015	1163	677, 615, 600	2500–1900		
Carbonates Hydroxides	ν_2	ν_3	ν_4			
Calcium Carbonate	876, 849	1458	714	2980–2500, 1794		
Calcium Hydroxide					3646	
Magnesium Hydroxide					3696	
Clinker phases		Unassigned Fundamentals				
C_3S	Si–O	935, 521		2000–1600		
C_2S	Si–O	991, 879, 847, 509		2060–1600		
C_3A	Al–O	889, 860, 812, 785, 762, 621, 586, 518, 506				
C_4AF	Fe–O	700–500				

2.0 MATERIALS AND MIXES

Fly ash (FA), *β*-cyclodextrin (*β*-CD) and Portland cement (CEM I 52.5 N) were the main materials in this study. The FA was obtained from Matla ESKOM power station, South Africa. *β*-CD from Wacker Chemie (Munich, Germany) was obtained from Industrial Urethanes (Pty) Ltd, South Africa. The cement type (CEM I 52.5N) was obtained from Pretoria Portland Cement Company (PPC), South Africa.

The composition of the FA and the cement used are presented in Table 2 and the *β*-CD composition is presented in Table 3. Twelve cement paste samples were prepared with a W/B of 0.3. The FA-*β*-CD mixtures were prepared by co-grinding a pre-weighed amount of *β*-CD and FA. FA was used in percentages of 30 and 50, while *β*-CD was used in 0.025, 0.05 and 0.1 percentages. These percentages were based on the total percentage of cement (by mass). The samples were labelled as described in Table 4. The percentages of *β*-CD used were based on the results of the indicative strength and durability tests that were published earlier by the authors [8, 9].

Table 2: Chemical composition of the fly ash and cement used

Content in oxide form.	% mass FA	% mass Cement
SiO_2	50.26	18.8
Al_2O_3	31.59	3.77
Fe_2O_3	3.08	3.83
MgO	2.04	1.68
CaO	6.78	66.70
Na_2O	0.56	0.09
K_2O	0.81	0.26
TiO_2	1.64	0.45
SO_3	0.55	4.53
LOI	1.42	-
SiO_2/Al_2O_3	1.59	-

86 **Table 3:** Characterisation of the β-cyclodextrin used

Property	β -CD
Empirical formula	$C_{42}H_{70}O_{35}$
Bulk density	400-700 kg/m^3
Solubility in water at 25 ^oC	18.5 g/l
Content (on dry basis)	Min. 95 %

87

88

89 **Table 4:** Description of samples used

SAMPLE	COMPOSITION	DESCRIPTION
a	Control (100% C)	Reference sample with cement
b	C30FA	Sample with cement and 30% fly ash
c	C50FA	Sample with cement and 50% fly ash
d	C0.025CD	Sample with cement and 0.025% β-cyclodextrin
e	C0.05CD	Sample with cement and 0.05% β-cyclodextrin
f	C0.1CD	Sample with cement and 0.1% β-cyclodextrin
g	C30FA0.025CD	Sample with cement and 30% fly ash-0.025% β-cyclodextrin
h	C30FA0.05CD	Sample with cement and 30% fly ash-0.05% β-cyclodextrin
i	C30FA0.1CD	Sample with cement and 30% fly ash-0.1% β-cyclodextrin
j	C50FA0.025CD	Sample with cement and 50% fly ash-0.025% β-cyclodextrin
k	C50FA0.05CD	Sample with cement and 50% fly ash-0.05% β-cyclodextrin
l	C50FA0.1CD	Sample with cement and 50% fly ash-0.1% β-cyclodextrin

90

91 The structure of the hydrated cement paste samples was studied by XRD and FT-IR. The
92 surface morphology of the hydrated samples was studied using SEM. For these tests, cement
93 paste samples were cast in 40 x 40 x 160 mm moulds and were covered with polythene and
94 left for 24 hours before demoulding. Samples with β-CD were left under polythene for 48
95 hours before demoulding. These samples were still soft and could not be handled after 24

hours. SANS 5861-3 [10], stipulated that due to retarding effect of a material such that the pre-demoulding time lapse of 20 to 24 hours is not suitable, the time may be extended for a suitable period. After the samples were demoulded, they were sliced into approximately 8 mm thick slices using a slow speed cut-off saw with a diamond-wafering blade. The sliced samples were well labelled and placed in a water bath maintained at 23 ^{o}C ± 2 ^{0}C for curing until the testing ages. At each testing age, a slice of each sample was placed in an excess of cold acetone for 2 hours to stop hydration. This time period was intended to facililitate acetone to completely be exchanged with the pore water. Acetone had been previously used by several researchers [11-15] to stop hydration. Since cyclodextrin is practically insoluble in acetone [16], the use of acetone to stop hydration had no effect on the stability of the cement paste.

After 2 hours in acetone, the samples were put in an oven maintained at 60 ^{0}C for a period of 24 hours to avoid hydrate decomposition. For XRD and FT-IR, the samples were then pulverised with a pestle in a porcelain mortar, sieved on a 75 μm sieve and kept in a desiccator, ready for testing. Samples were tested after 24 hours, 7 days, 28 days and 90 days hydration periods. The XRD samples were prepared using the front loading technique. For SEM, the samples, after being removed from the oven were put in a desiccator and tested after 7 days, 28 days and 90 days hydration periods. Immediately prior to testing, the samples were broken to reveal fresh surfaces for examination.

3.0 EXPERIMENTAL PROCEDURE

3.1 X-ray diffraction (XRD)

XRD analysis was done to determine the minerals present in the powdered samples using a PW1710 Philips powder diffractometer with monochromatic Cu Kα radiation at 40 kV and

40 mA. Diffractograms were collected over a range of 2θ between 10-80^{o}, with a step size of 0.017. The XRD samples were prepared using the front loading technique. The test was done at the chemistry laboratories of the University of Johannesburg.

3.2 Scanning electron microscope (SEM)

The twelve samples were subjected to scanning electron microscopy (SEM) (PHILIPS Environmental Scanning Electron Microscope XL30). The samples were mounted on the SEM and irradiated with a beam of electrons at 15 kV.

3.3 Fourier transform-infrared analysis (FT-IR)

FT-IR analysis was done using a Perkin Elmer 100 Spectrometer incorporated with diamond attenuated total reflectance (ATR). The diamond ATR instrument was installed securely on the spectrometer. The samples were analysed in their powder form using a ZnSe/diamond composite as the key component of the universal ATR sample holder with the characteristic peaks in wavenumbers from 650 to 4000 cm^{-1}. Spectra were collected and recorded with nitrogen gas at 20 ml/min flow rate and a temperature range between 30 and 800 ^{0}C at 10.00 ^{0}C/min. The test was done at the chemistry laboratories of the University of Johannesburg.

4.0 RESULTS AND DISCUSSIONS

4.1 XRD

4.1.1 XRD analysis after 24 hours hydration period

XRD was used to monitor the evidence and extent of hydration in the samples by studying the consumption of the crystalline anhydrous phases of the samples (C_3S, C_2S, C_3A and C_4AF), the formation of the crystalline hydrates (CH) and the formation of amorphous C–S–H (this is indicated by the change from the crystalline anhydrous phases to amorphous phases

144 of the diffractogram). The most prominent crystalline peaks observed after 24 hours
145 hydration, as shown in Figure 1(a-l), were of calcium hydroxide (CH), tricalcium silicate
146 (C_3S) and dicalcium silicate (C_2S). Quartz (SiO_2) and mullite ($Al_6Si_2O_{13}$) were evident in
147 samples containing FA (Figure 1 b, c, g, h, i, j, k, l). A little peak of cyclodextrin (CD) was
148 observed in some of the samples containing *β*-CD (Figure 1 e, f, h, i, j, k, l).
149
150 It is evident from Figure 1(e, f, h, i, k, l) that the samples with 0.05CD and 0.1CD had a
151 higher C_3S/C_2S intensity than other samples. The peaks observed for the control sample
152 (Figure 1a) are similar to those reported by other researchers [3, 5, 11, 17-19]. Delayed
153 hydration was evident for samples containing *β*-CD (Figure 1d, e, f, g, h, i, j, k, l) at the 24
154 hour hydration period, as seen from the high content of C_3S and C_2S and little formation of
155 CH at the region approximately 18.3^0 as compared to the control sample. As expected, the
156 pozzolanic reaction was slow, therefore at this hydration stage, formation of CH was still in
157 process so no consumption of CH by FA was observed. Further delay in the formation of CH
158 was observed for C50FA and FA-*β*-CD composites samples relative to the C30FA sample.
159 The higher the content of FA and *β*-CD, the lower the formation of CH observed, which
160 might be as a result of the dilution effect. The addition of FA reduced the clinker content and
161 therefore less CH developed.
162
163
164
165
166
167
168

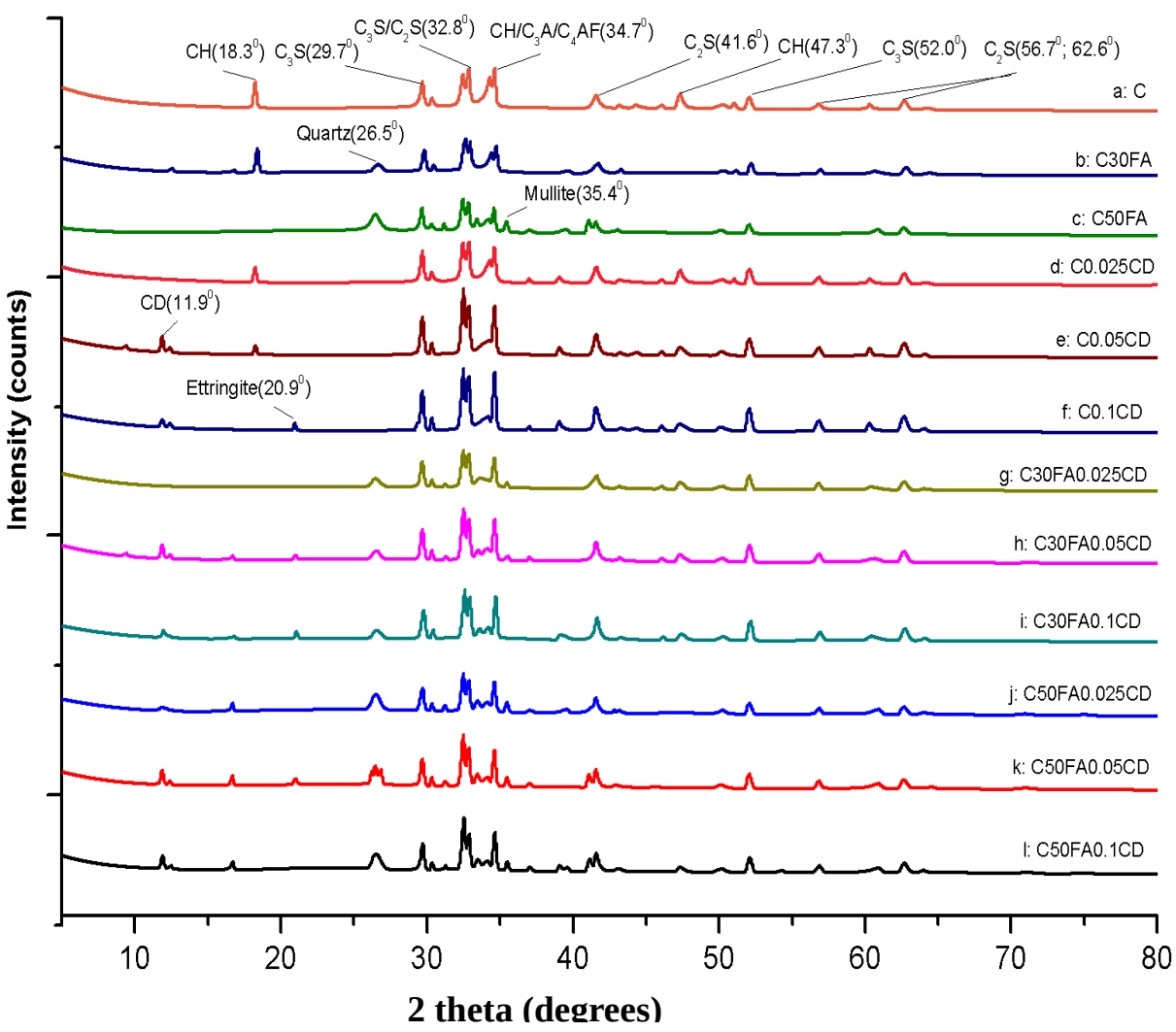

Figure 1: X-ray diffractograms (XRD) of cement paste samples hydrated for 24 hours

4.1.2 XRD analysis after 7 days hydration period

Figure 2(a-l) shows the diffractograms of the cement paste samples hydrated for 7 days. At this hydration period, the intensity of C_3S and C_2S peaks were reduced for all the samples due to the formation of calcium silicate hydrate gel (C-S-H) and calcium hydroxide (CH), as is evidenced by a high peak for CH. *β*-CD increased the dissolution of C_3S and C_2S and aided the formation of CH (Figure 2d, e, g, h, j, k) and amorphous C-S-H at 0.025% and 0.05% *β*-CD replacements compared to the control, C30FA and C50FA samples. These samples

(samples containing 0.025% and 0.05% β-CD) are envisaged to have an increased strength at this early hydration period following the observation reported by Khater [15] that an increased early formation of C-S-H would lead to an increase in strength. A higher growth rate of the hydrates (CH) was observed for the samples with 0.025% β-CD than for the samples with 0.05% β-CD.

A lower formation of CH was observed in the samples with 0.1% β-CD replacement (Figure 2f, i, l) compared to the 0.025% and 0.05% β-CD replacements samples. This observation for the 0.1% β-CD replacement samples might be an indication of setting retardation, which will result in a delay of early formation of hydration products. Slower pozzolanic reaction was observed in the FA and FA-β-CD composite samples (Figure 2b, c, g, h, i, j, k, l). A higher content of quartz and crystalline phase of mullite was observed in samples containing 50% FA (Figure 2c, j, k, l).

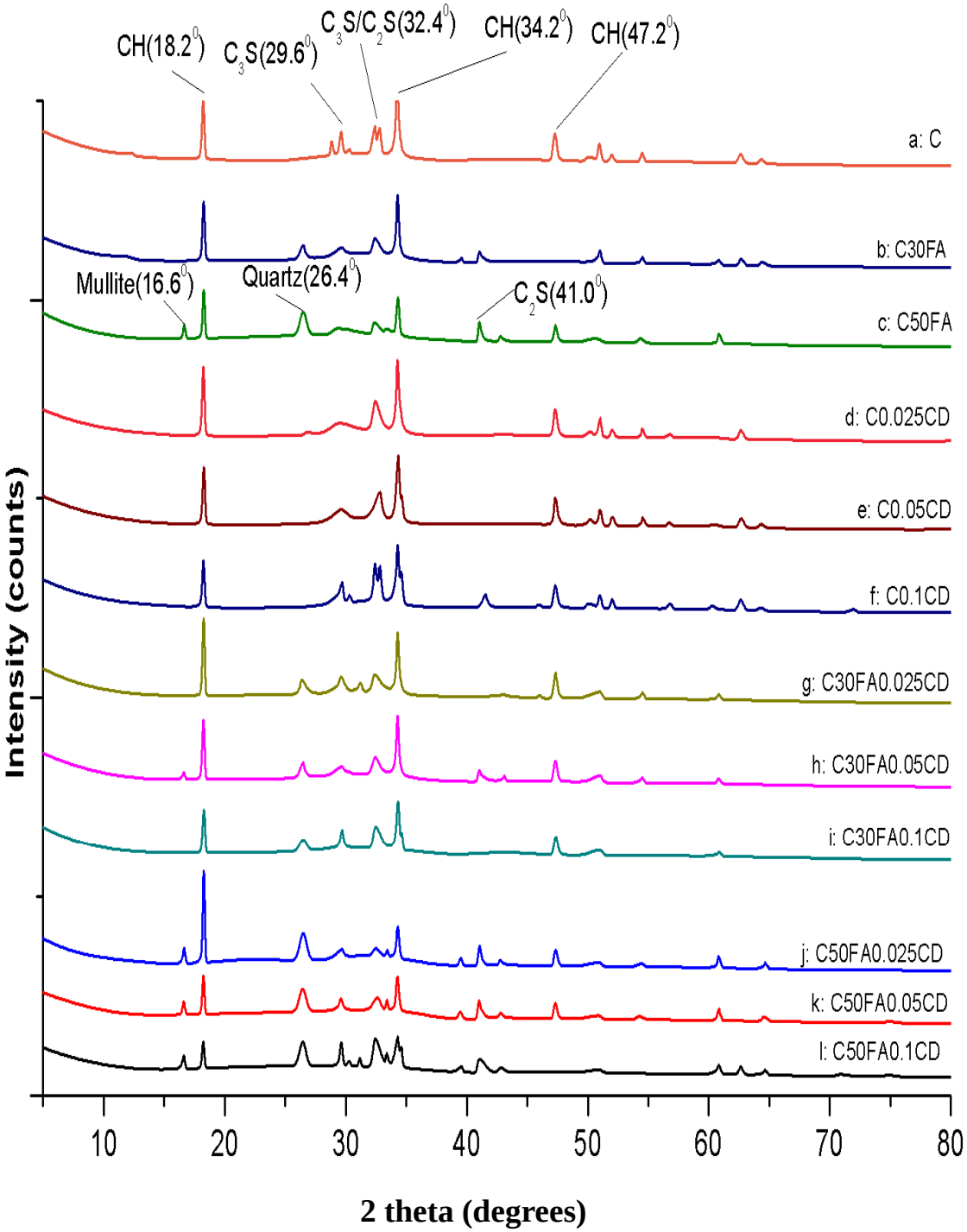

Figure 2: X-ray diffractograms (XRD) of cement paste samples hydrated for 7 days

4.1.3 XRD analysis after 28 days hydration period

The diffractograms of the cement paste samples hydrated for 28 days are shown in Figure 3(a-l). In all the samples, the crystalline anhydrous phases were further consumed at the 28

days hydration period to form more amorphous C–S–H. There was little difference between the levels of dissolution of anhydrous phases in the control sample (Figure 3a) compared to samples with *β*-CD (Figure 3d, e, f). The reduction of the CH peak in all the FA and FA-*β*-CD composite samples (Figure 3b, c, g, h, i, j, k, l) at the 28 days hydration period compared to the 7 days hydration period was evidence of pozzolanic reaction, which allowed the consumption of some of the CH to produce more C-S-H. The higher the FA content, the greater the reduction in the CH peak observed.

Further dissolution of silica in FA and FA-*β*-CD composite samples at 28 days hydration, as compared to 7 days hydration period, confirmed that pozzolanic reaction was taking place between the SiO_2 and calcium hydroxide (CH). Higher contents of quartz (compared to the samples containing 30% FA) and mullite were still left in samples containing 50% FA (Figure 3c, j, k, l).

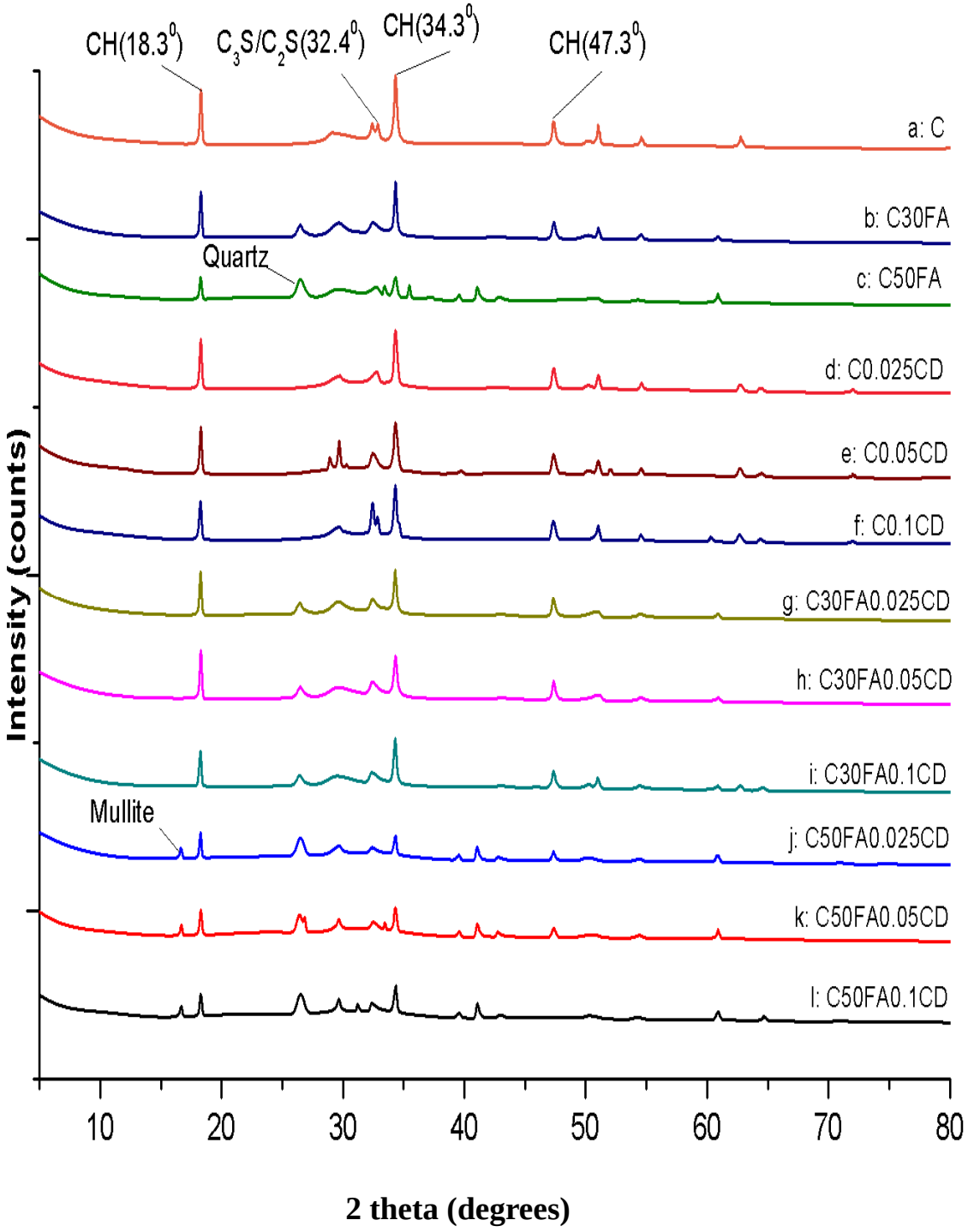

Figure 3: X-ray diffractograms (XRD) of cement paste samples hydrated for 28 days

4.1.4 XRD analysis after 90 days hydration period

Hydration reaction was envisaged to have been completed by 90 days. The diffractograms of the cement paste samples at this hydration period are presented in Figure 4 (a-l). The

anhydrous phases of cement compounds have completely formed crystalline CH and amorphous C-S-H (Figure 4a, d, e, f). The higher formation of CH and greater dissolution of the anhydrous phases observed in β-CD samples (Figure 4d, e, f), as compared to the control sample (Figure 4a), are evidence that the β-CD aided the hydration reaction. A greater CH peak was observed for samples with 0.025% β-CD (Figure 4d) than the other samples.

At the 90 days hydration period, a greater pozzolanic reaction had taken place in the FA samples resulting in a reduction of the CH peak (Figure 4b, c). A higher content of FA resulted in a greater consumption of CH. Reduced CH peaks were also observed for the FA-β-CD composite samples containing 0.05% and 0.1% β-CD replacements (Figure 4h, i, k, l) at 90 days hydration period, compared to 28 days hydration period as a result of the pozzolanic reaction. At 0.025% β-CD replacements in the FA-β-CD composite samples (Figure 4g, j), increased CH peaks (at approximately 18.3^0) were observed, especially for the sample with 50% FA at 90 days hydration period compared to 28 days hydration period. The 0.025% β-CD replacements had little effect on the pozzolanic reaction.

In general, the XRD results showed the changes that occurred in the phases as hydration progressed. Highly crystalline anhydrous phases in the 24 hours hydration samples gradually formed the hydration products phases (CH and C-S-H). β-CD showed a delay in the 24 hours hydration, which was an indication of the retarding effect of the β-CD. Early hydration reaction was observed for control samples from the 24 hours hydration period. β-CD generally improved the hydration reaction of the control sample from the 7 days hydration period. The effect of β-CD on pozzolanic reaction was revealed from the 28 days hydration period. The 0.025% β-CD had little effect on pozzolanic reaction.

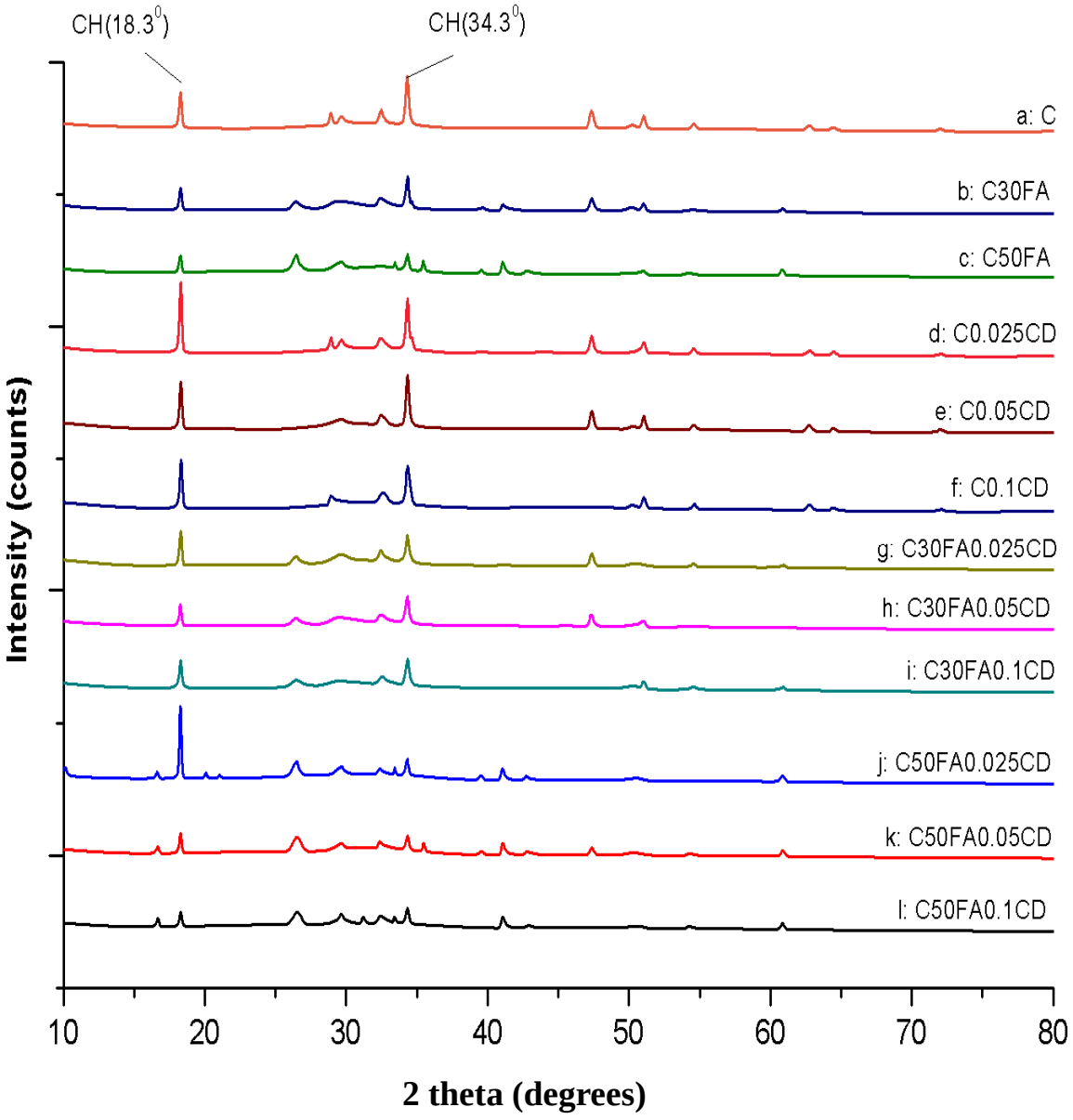

312 **Figure 4:** X-ray diffractograms (XRD) of cement paste samples hydrated for 90 days

313

314 **4.2 SEM**

315 **4.2.1 SEM analysis after 7 days hydration period**

316 At the 7 days hydration period, hydration reaction would have started while pozzolanic
317 reaction was still delayed as seen in the XRD results. Figure 5(a-l) shows the SEM
318 micrograghs of cement paste samples hydrated for 7 days. The control sample (Figure 5a)

showed a spongy structure, revealing early formation of C-S-H with smaller particles coagulating together around unhydrated cement grains. Some pockets of capillary pores were also revealed. Unhydrated spherical particles of FA are shown in the C30FA sample (Figure 5b). At lower magnification, which is inserted, evidence of tiny needle shaped ettringite formation can be seen. The C50FA sample (Figure 5c) showed a semi-amorphous structure with more obvious and brighter evidence of needle-like-shaped ettringite at lower magnification (inserted).

The formation of primary crystalline structure of portlandite (CH) is evident in the C0.025CD sample (Figure 5d); a better view can be seen in lower magnification (inserted). This confirms the XRD observation for samples containing 0.025% β-CD (Figure 2d), which showed a greater peak of CH at 7 days hydration compared to the control sample. A cloudy surface was also observed for this sample, which is attributed to the adsorption of β-CD at the surface of the hydrates. With the 0.05% β-CD sample (Figure 5e), more evidence of cloudy surface was seen, with coagulation of tiny particles revealing early formation of C-S-H, due to the dissolution of the anhydrous phase of the cement paste. The cement paste sample containing 0.1% β-CD (Figure 5f) revealed a semi-amorphous surface revealing unhydrated cement grains, with lower evidence of hydration products in this sample compared to 0.025% and 0.05% β-CD samples. These observations confirmed the XRD results.

For the FA-β-CD composite samples, layered deposition of stacked CH primary crystals was observed for C30FA0.025CD sample (Figure 5g) with early micro crystalline C-S-H formation around the FA particles. Breaking of FA particles into a flaky/spongy like structure was observed in the C30FA0.05CD sample (Figure 5h), revealing improved reaction between FA and the hydrates. Improved flaky/spongy, less compacted like structure, with evidence of

unhydrated particles of cement grains and FA can be seen in C30FA0.1CD sample (Figure 5i).

The C50FA0.025CD sample (Figure 5j) revealed coagulation of particles with little evidence of hydration products. The cloudy surface showing the adsorption of β-CD and FA on the surface of the hydrates is shown for C50FA0.05CD sample (Figure 5k). Unhydrated cement grains and FA particles with larger capillary pore were revealed for the C50FA0.1CD sample (Figure 5l).

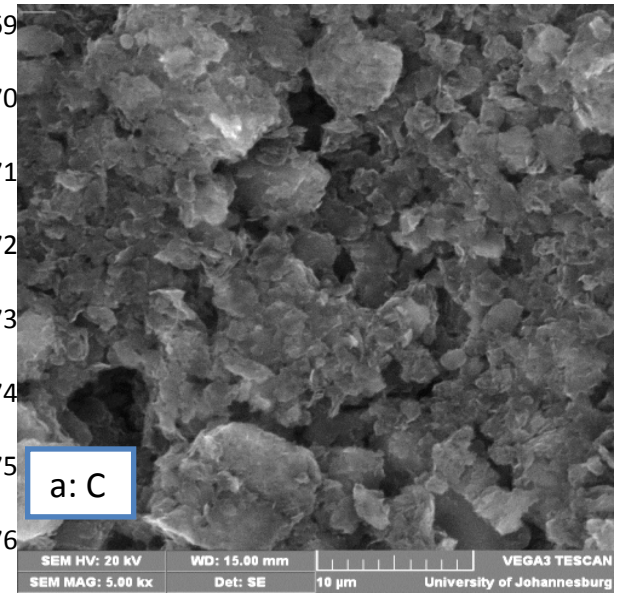
a: C
SEM HV: 20 kV
WD: 15.00 mm
VEGA3 TESCAN
SEM MAG: 5.00 kx
Det: SE
10 µm
University of Johannesburg

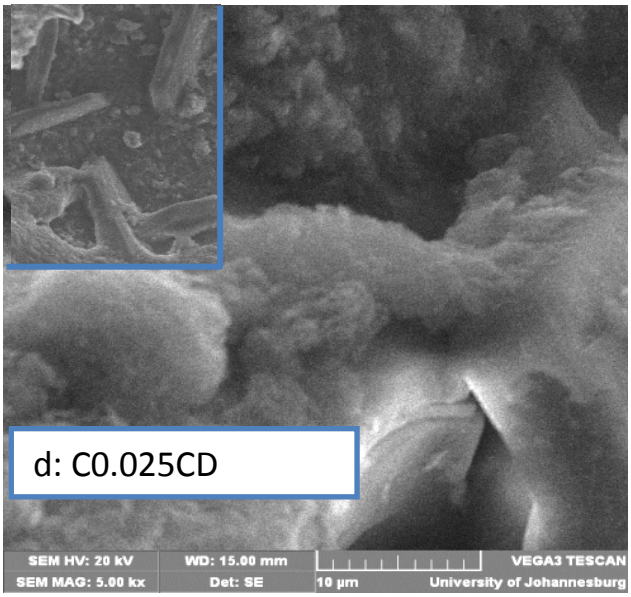
d: C0.025CD
SEM HV: 20 kV
WD: 15.00 mm
VEGA3 TESCAN
SEM MAG: 5.00 kx
Det: SE
10 µm
University of Johannesburg

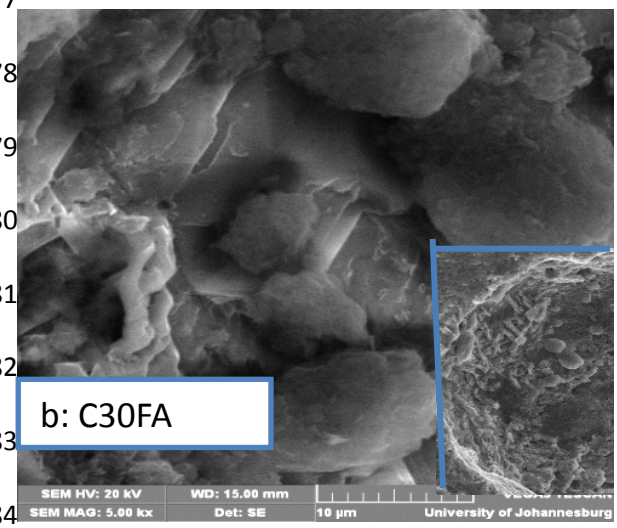
b: C30FA
SEM HV: 20 kV
WD: 15.00 mm
SEM MAG: 5.00 kx
Det: SE
10 µm
University of Johannesburg

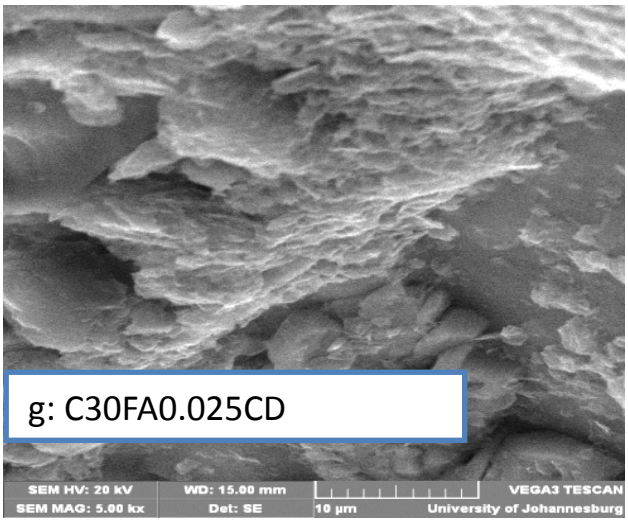
g: C30FA0.025CD
SEM HV: 20 kV
WD: 15.00 mm
VEGA3 TESCAN
SEM MAG: 5.00 kx
Det: SE
10 µm
University of Johannesburg

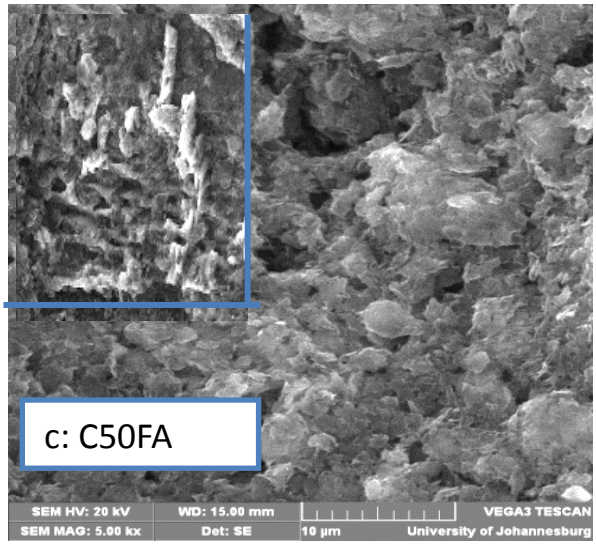
c: C50FA
SEM HV: 20 kV
WD: 15.00 mm
VEGA3 TESCAN
SEM MAG: 5.00 kx
Det: SE
10 µm
University of Johannesburg

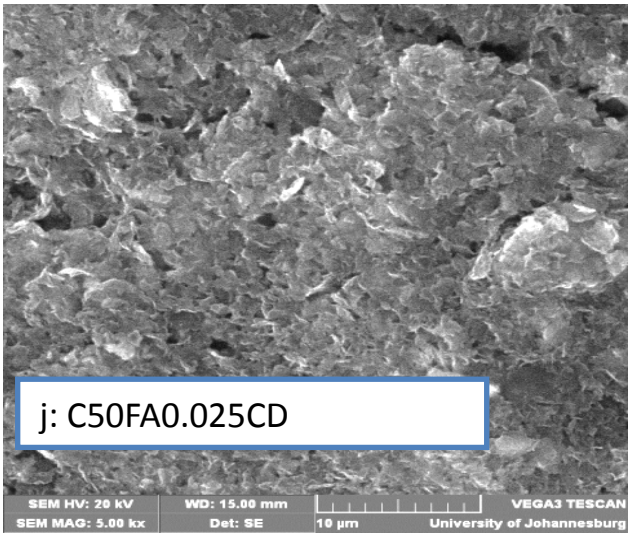
j: C50FA0.025CD
SEM HV: 20 kV
WD: 15.00 mm
VEGA3 TESCAN
SEM MAG: 5.00 kx
Det: SE
10 µm
University of Johannesburg

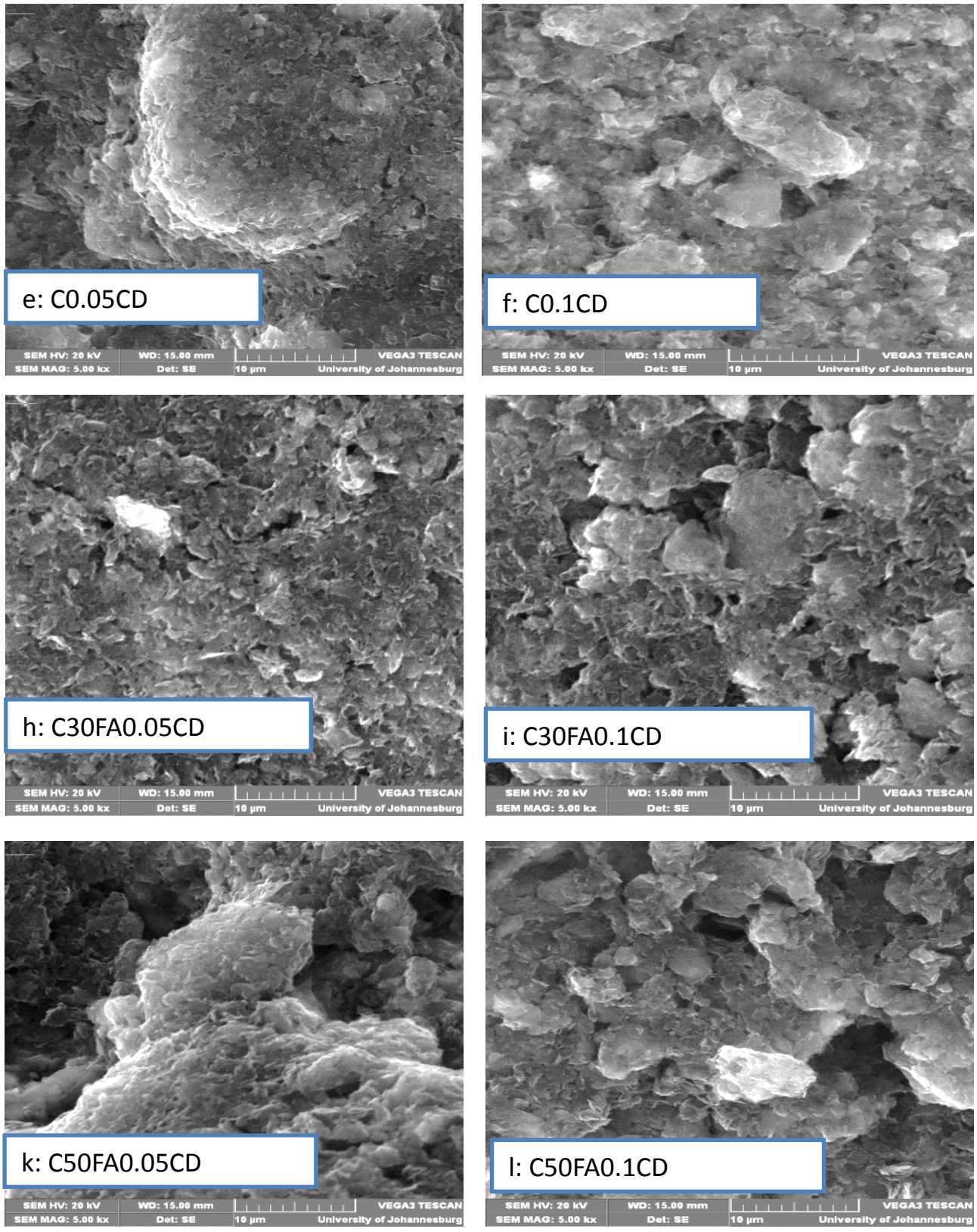

Figure 5: SEM of samples (a-l) hydrated for 7 days at 5000x magnification

4.2.2 SEM analysis after 28 days hydration period

The SEM micrographs of the samples hydrated for 28 days are shown in Figure 6(a-l). Denser morphology structures were observed for all the samples revealing improved hydration and pozzolanic reactions. Formation of C-S-H gel, which filled the pores and resulted in a more dense surface and compact particles was observed for the control sample (Figure 6a), especially at lower magnification (inserted). Breaking of FA particles, resulting in smaller particle sizes and a denser surface was evidence of pozzolanic reaction as seen in the C30FA sample (Figure 6b). Less crystalline structure revealed the gradual formation of C-S-H gel. A spongy, less compacted structure was observed for the C50FA sample (Figure 6c) revealing a slower pozzolanic reaction than for the C30FA sample.

More improved denser surfaces were observed for samples containing β-CD (Figure 6d, e, f) when compared to control sample (Figure 6a). The improved denser surface of β-CD samples revealed greater hydration reaction at this hydration period than at 7 days. A less compacted surface was revealed for the C0.1CD sample (Figure 6f) than for the C0.025CD and C0.05CD samples (Figure 6 d, e). Reduced cloudy surfaces showing that more of β-CD and FA have been utilized in the reaction were observed for all FA-β-CD composite samples (Figure 6g, h, i, j, k, l) than 7 days hydration samples. This revealed improved pozzolanic reactions. The C30FA0.05CD sample (Figure 6h) showed a denser and more compact particle structure than the C30FA0.025CD and C30FA0.1CD samples (Figure 6g, i). Improved pozzolanic reaction showing the transformation of FA particles into the hydrate was obvious in the C50FA0.025CD sample (Figure 6j). The C50FA0.05CD and C50FA0.1CD samples (Figure 6k, l) showed similar features of spongy morphology revealing gradual formation of C-S-H. The C50FA0.05CD sample (Figure 6k) was more compacted than the C50FA0.1CD sample (Figure 6l).

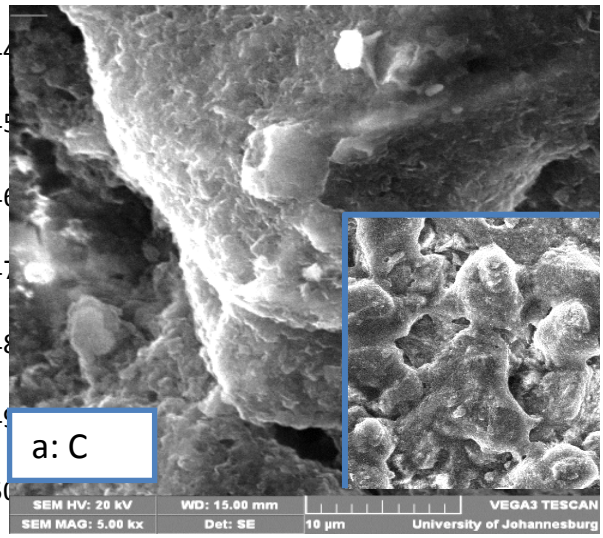
a: C
SEM HV: 20 kV
WD: 15.00 mm
VEGA3 TESCAN
SEM MAG: 5.00 kx
Det: SE
10 µm
University of Johannesburg

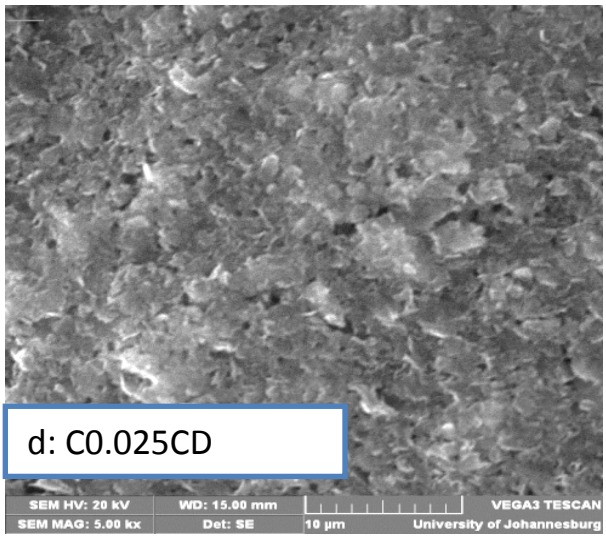
d: C0.025CD
SEM HV: 20 kV
WD: 15.00 mm
VEGA3 TESCAN
SEM MAG: 5.00 kx
Det: SE
10 µm
University of Johannesburg

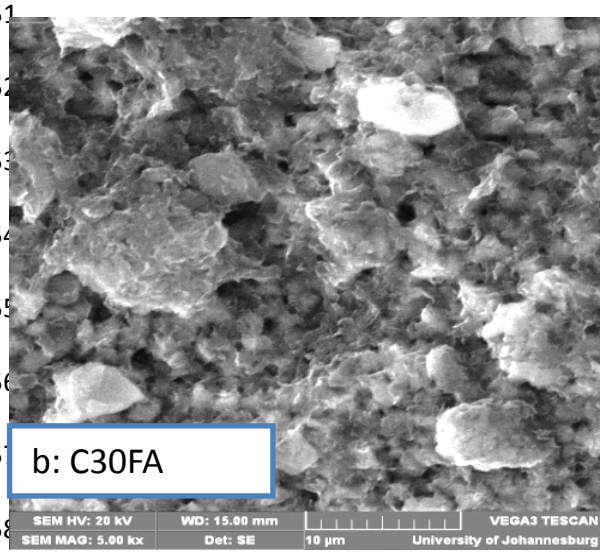
b: C30FA
SEM HV: 20 kV
WD: 15.00 mm
VEGA3 TESCAN
SEM MAG: 5.00 kx
Det: SE
10 µm
University of Johannesburg

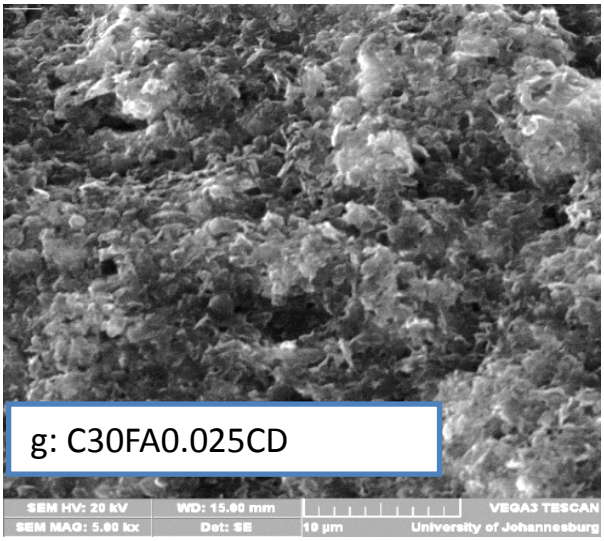
g: C30FA0.025CD
SEM HV: 20 kV
WD: 15.00 mm
VEGA3 TESCAN
SEM MAG: 5.00 kx
Det: SE
10 µm
University of Johannesburg

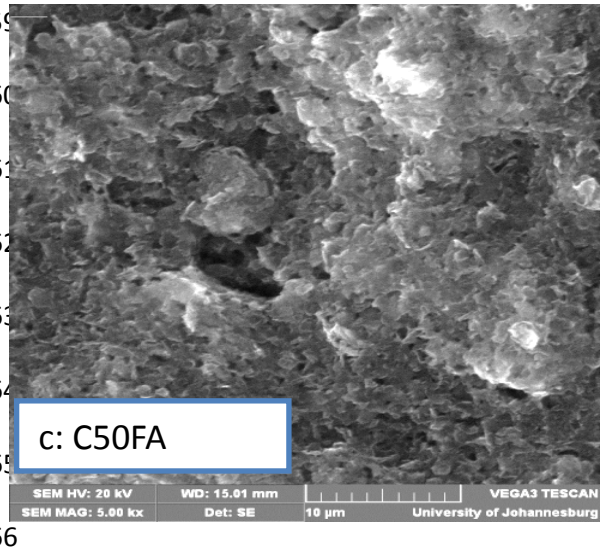
c: C50FA
SEM HV: 20 kV
WD: 15.01 mm
VEGA3 TESCAN
SEM MAG: 5.00 kx
Det: SE
10 µm
University of Johannesburg

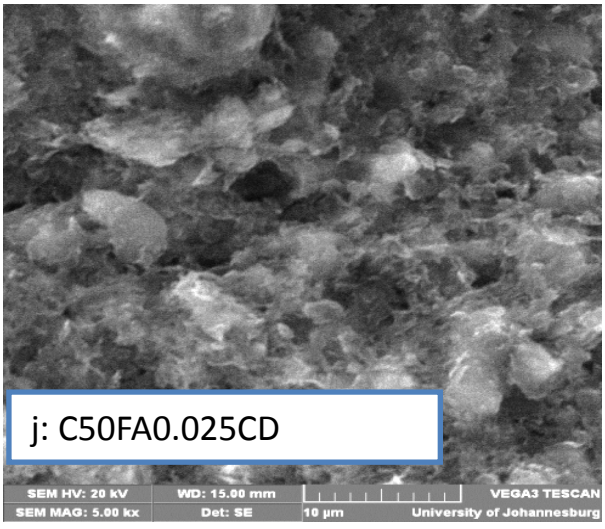
j: C50FA0.025CD
SEM HV: 20 kV
WD: 15.00 mm
VEGA3 TESCAN
SEM MAG: 5.00 kx
Det: SE
10 µm
University of Johannesburg

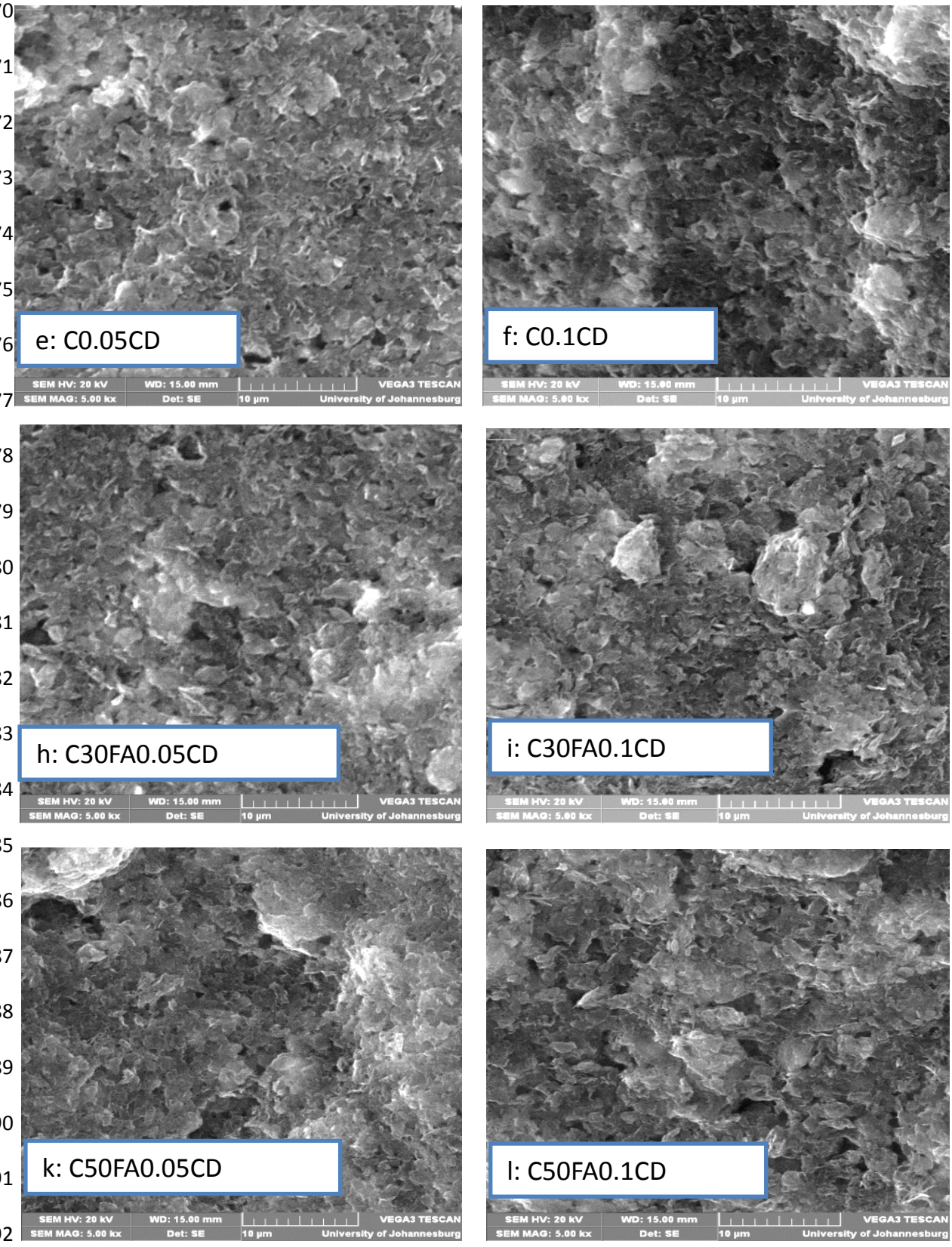

Figure 6: SEM of samples (a-l) hydrated for 28 days at 5000x magnification

494 **4.2.3 SEM analysis after 90 days hydration period**

495 Well hydrated morphology was revealed for all the samples after 90 days hydration period as
496 shown in Figure 7 (a-l). The control sample's morphology (Figure 7a) showed flowered flaky
497 particles that have been coagulated together; no further hydration reaction process was
498 evident. Capillary pores were also shown. More flaky particles with evidence of some C-S-H
499 gel covering the particles were revealed for the C30FA sample (Figure 7b). Reduced
500 capillary pores are evident in the C30FA sample compared to the control sample. Large
501 particles undergoing further pozzolanic reaction are seen in the morphology of the C50FA
502 sample (Figure 7c).

503

504 The samples containing β-CD (Figure 7d, e, f) showed an improved denser surface and
505 reduced continuous capillary pores compared to the control sample (Figure 7a). A more
506 improved surface was revealed for the C0.025CD sample (Figure 7d). The C0.05CD sample
507 (Figure 7e) showed greater flaky particles morphology than the C0.025CD and C0.1CD
508 samples, these flaky particles were better packed than for the control sample. The C0.1CD
509 sample (Figure 7f) showed evidence of C-S-H gel covering the particles. This could be
510 attributed to the increased amount of β-CD in C0.1CD sample, which showed evidence of
511 delayed hydration.

512

513 Compacted morphologies are seen for C30FA0.025CD and C30FA0.05CD composite
514 samples (Figure 7g, h). A less compacted, porous flaky morphology was revealed for the
515 C30FA0.1CD sample (Figure 7i). Reduced particle sizes were observed for the
516 C30FA0.05CD sample (Figure 7h) than for the C30FA, C30FA0.025CD and C30FA0.1CD
517 samples (Figure 7 b, g, i). Evidence of C-S-H gel was seen on the surface of C50FA0.025CD
518 and C50FA0.05CD composite samples (Figure 7 j, k) particles. The dissolving surface of the

C50FA0.025CD and C50FA0.05CD samples was evidence of the delayed pozzolanic reaction of the FA-*β*-CD composite samples with 50% FA compared to the FA-*β*-CD composite samples with 30% FA. An improved denser surface was observed for respective FA-*β*-CD composite samples when compared to their original C30FA and C50FA samples.

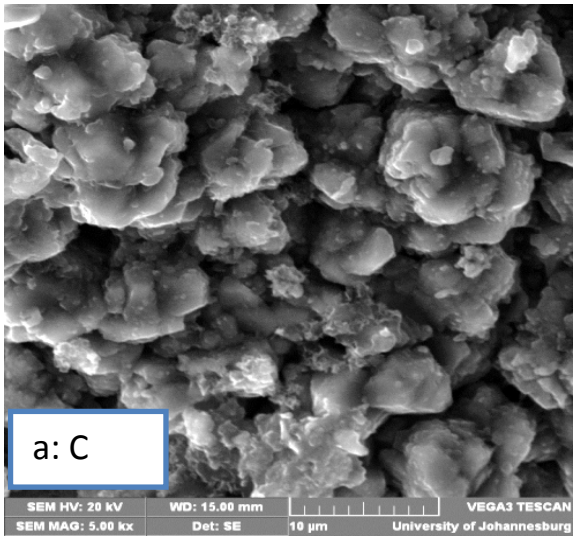

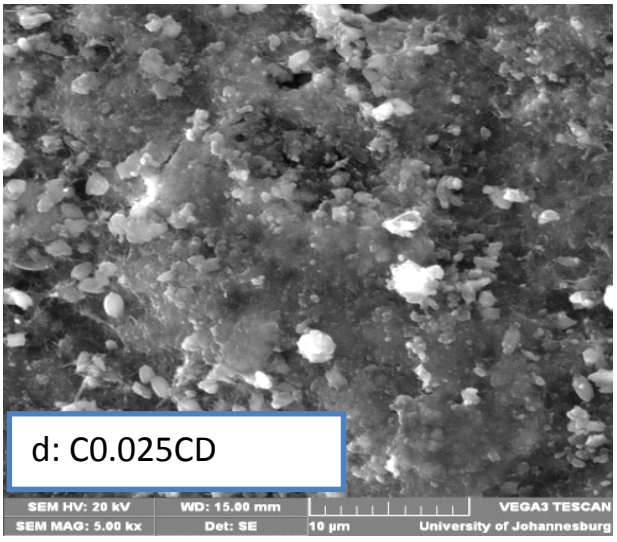

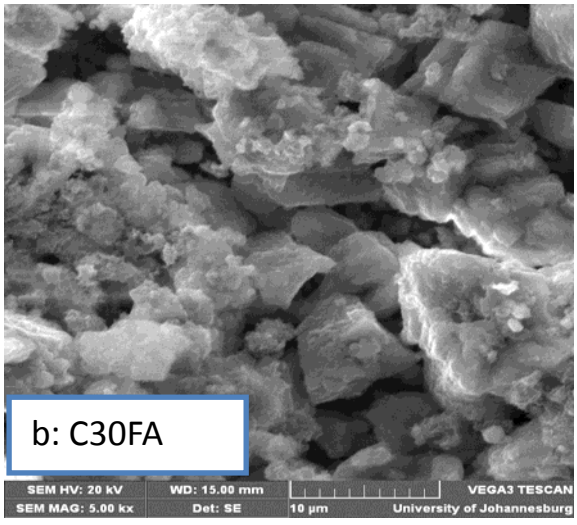

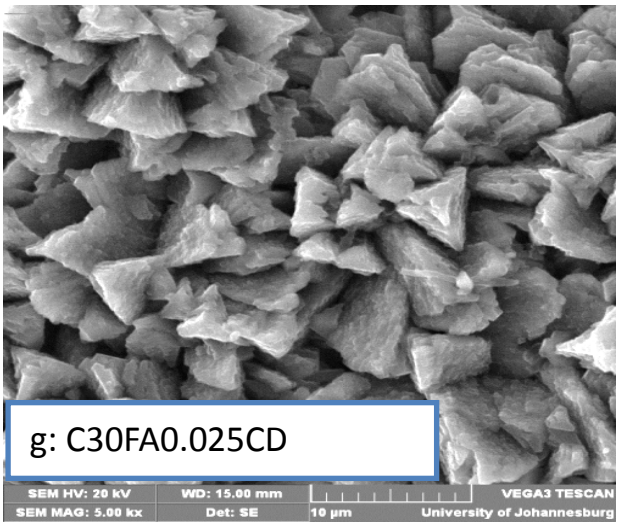

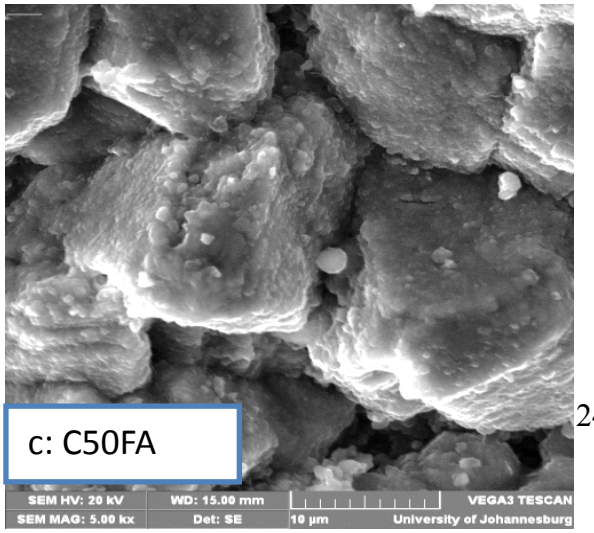

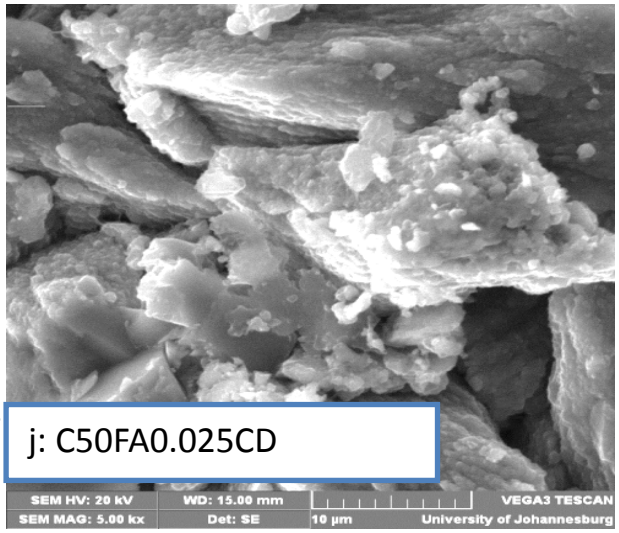

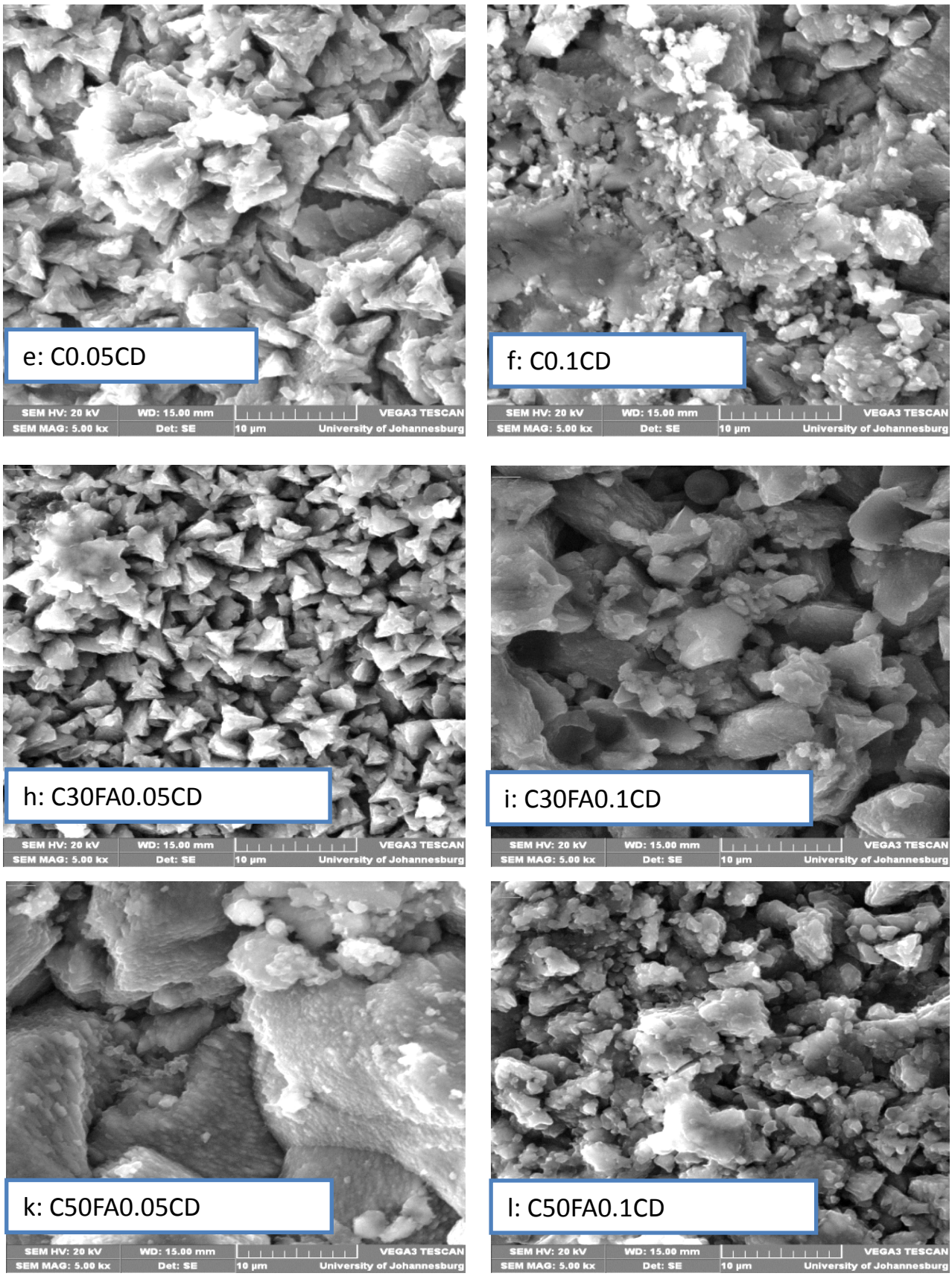

Figure 7: SEM of samples (a-l) hydrated for 90 days at 5000x magnification

566 **4.3 FT-IR**

567 **4.3.1 FT-IR analysis after 24 hours hydration period**

568 The FT-IR spectra of the samples hydrated for 24 hours are shown in Figure 8(a-l). The
569 control sample (Figure 8a) showed Si-O asymmetric stretching band (υ_3) at 962 cm^{-1} due to
570 the dissolution of C_3S clinker phase and at 876 cm^{-1} due to the dissolution of C_2S clinker
571 phase [7, 20-22]. At 1119 cm^{-1}, the band due to the υ_3 vibration of the SO_4^{2-} group in
572 sulphates (gypsum) [7, 23] was observed in the control sample (Figure 8a). As hydration
573 progresses, this region is expected to be absorped by the υ_3 vibration of SiO_4^{2-}, therefore,
574 leaving υ_3 vibration of the SO_4^{2-} to be obscured [20, 23-24]. The peak at 1416 cm^{-1} and
575 overtone at 2945 cm^{-1} correspond to the CO_3 from calcium carbonate [7, 23] and they also
576 coincide with one of the υ_3 vibration of SiO_4^{2-} [21]. As hydration progresses, the CO_3 band
577 peak is expected to decrease [23] while υ_3 vibration of SiO_4^{2-} increases, therefore, any peak
578 at the region 1420 cm^{-1} – 1490 cm^{-1}, at further hydration period will be assigned to υ_3
579 vibration of SiO_4^{2-}. The expected prominent peaks upon hydration and setting are the strong
580 band due to CO_3/ SiO_4^{2-} and small sharp OH stretching band [20]. In pozzolanic reaction, the
581 small sharp OH stretching band will be consumed.

582

583 The peak at 2174 cm^{-1} of control sample is attributed to asymmetric stretching of Si–O–Si in
584 the silicate framework structures [25]. The peaks observed for control sample are similar to
585 what had been reported previously by other researchers [7, 20-23]. The XRD results at this
586 hydration period reported in this study revealed prominent peaks of C_3S and C_2S (Figure 1a)
587 and confirmed the FT-IR result for the control sample. It has been reported that the shift of
588 the Si–O asymmetric stretching vibration to higher wavenumbers due to the polymerisation
589 of the SiO_4^{2-} units during C–S–H formation is an indication of improved hydration reaction
590 [20, 24, 26, 27]. Delayed hydration reaction at the 24 hour hydration period was evident in all

591 samples with FA, β-CD and FA-β-CD composite (Figure 8b - l) due to the shift of the Si–O
592 asymmetric stretching vibration to lower wavenumbers. Broader and greater intensities of Si-
593 O asymmetric stretching bands (υ_3) were observed for C30FA and C50FA samples (Figure
594 8b, c) at lower wavenumbers compared to the control sample. This might be attributed to the
595 dissolution of C_3S and contribution of the higher content of SiO_2 in FA. The higher the
596 content of FA, the broader the Si-O asymmetric stretching band observed. Greater shift to
597 lower wavenumbers of υ_3 vibration of the SO_4^{2-} group at 1116 cm^{-1} and 1100 cm^{-1} for C30FA
598 and C50FA samples, respectively, also confirmed delayed hydration/pozzolanic reaction
599 effect of FA. As expected, the intensity of the CO_3 peak at 1446 cm^{-1} and 1439 cm^{-1} for
600 C30FA and C50FA samples respectively were reduced due to the reduced quantity of cement
601 used for these samples.
602
603 β-CD aided the dissolution of C_3S clinker phase resulting in the greater and sharper intensity
604 of Si-O asymmetric stretching band (υ_3) of samples containing β-CD (Figure 8d, e, f)
605 compared to the control sample. The higher the content of β-CD, the greater the Si-O
606 asymmetric stretching band (υ_3) intensity observed. The shift to lower wavelength of Si-O
607 asymmetric stretching band of samples containing β-CD showed that the dissolved C_3S was
608 not yet ready for hydration reaction at this hydration period, resulting in delayed hydration as
609 revealed in XRD results (Figure 1d, e, f). Greater intensity of υ_3 vibration of the SO_4^{2-} group
610 for samples containing β-CD (Figure 8d, e, f) also confirmed delayed hydration reaction for
611 these samples at the 24 hour hydration period. The higher the β-CD content, the greater the
612 intensity of υ_3 vibration of the SO_4^{2-} group and the greater the delay in hydration reaction
613 envisaged.
614

615 The FA-β-CD composite samples (Figure 8g, h, i, j, k, l), revealed sharpness of Si-O
616 asymmetric stretching band as compared to their respective original C30FA and C50FA
617 samples (Figure 8b, c). This observation is in agreement with the XRD results. It was
618 observed from the XRD results that FA-β-CD composite samples exhibited higher contents of
619 C_3S and C_2S at the 24 hour hydration period than the C30FA and C50FA samples (Figure 1g,
620 h, i, j, k, l). This indicated that a further delay of the hydration reaction at this hydration
621 period might be experienced for FA-β-CD composite samples when compared to their
622 respective original C30FA and C50FA samples. Further evidence of delayed hydration at the
623 24 hour hydration period is the sharpness of the υ_3 vibration of the SO_4^{2-} group for FA-β-CD
624 composite samples (Figure 8g, h, i, j, k, l) when compared to their respective original C30FA
625 and C50FA samples (Figure 8b, c).
626
627

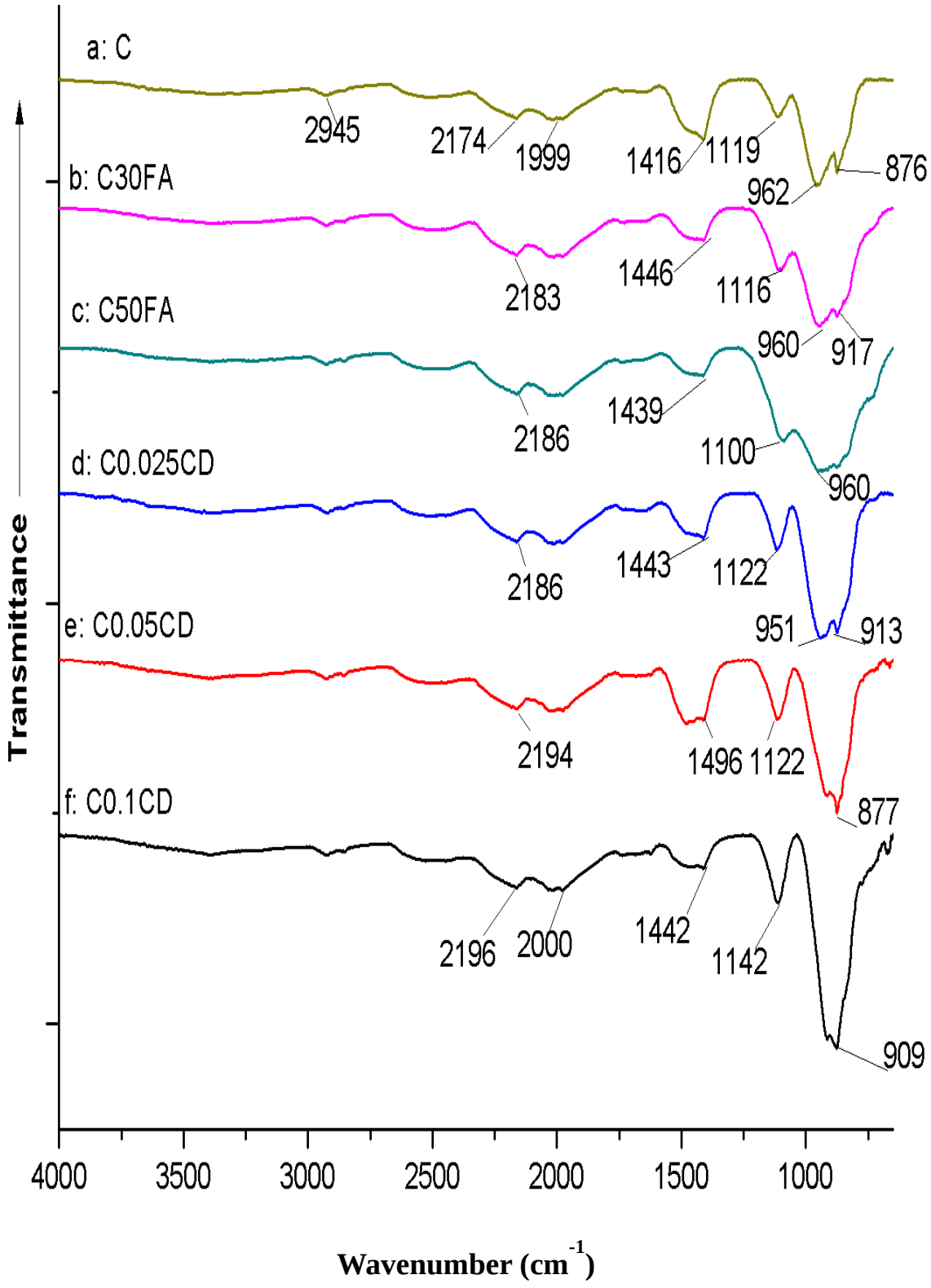

*Binary samples (24 hours hydration)

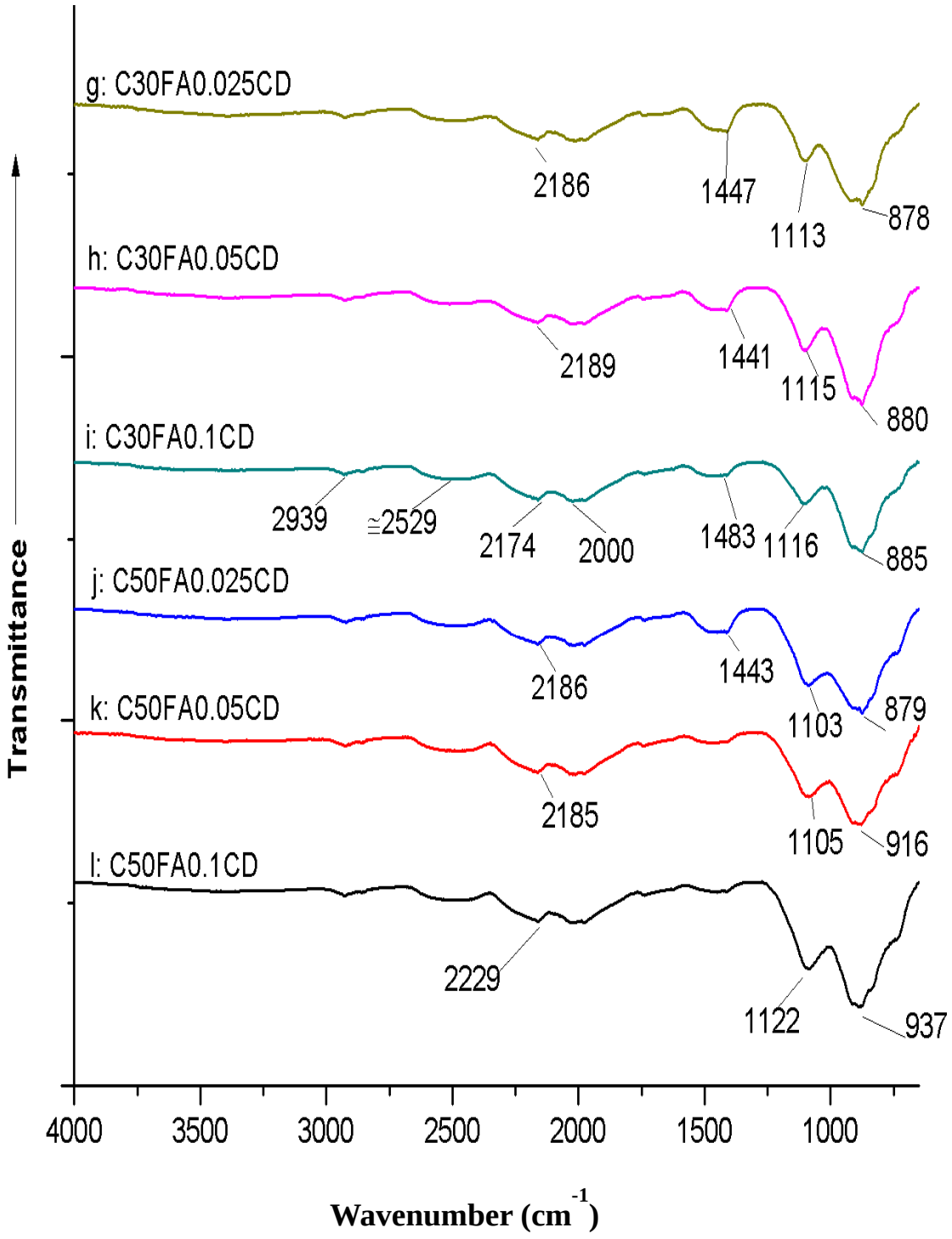

672 *Ternary samples (24 hours hydration)

673 **Figure 8:** FT-IR spectra of cement paste of binary and ternary samples hydrated for 24 hours

4.3.2 FT-IR analysis after 7 days hydration period

A degree of hydration reaction and pozzolanic reaction was revealed in all the samples hydrated for 7 days (Figure 9a-l). Reduced intensity and shift to higher wavelength of υ_3 vibration of the SO_4^{2-} group at 1132 cm^{-1} is evidence that, at this hydration period, the hydration reaction had started for the control sample (Figure 9a). The peak at 3644 cm^{-1}, attributed to the OH-stretch from $Ca(OH)_2$ also confirmed the hydration reaction for the control sample at the 7 days hydration period. This result confirmed the XRD result, where at the 7 days hydration period, reduced intensity of C_3S and C_2S peaks (Figure 2a), showing dissolution of these phases during hydration reaction was observed for the control sample compared to the 24 hours hydrated sample. It would be inconclusive to assign the peak at approximately 1424 cm^{-1} to either the CO_3 band or υ_3 vibration of SiO_4^{2-} at this hydration period, because both will have an influence at this age and it will be difficult to distinguish the effect of each of them. As hydration continues (28 days), the peak at this region will be assigned to the υ_3 vibration of SiO_4^{2-}.

Greater intensity of Si-O asymmetric stretching bands (υ_3) was observed for C30FA and C50FA samples (Figure 9b, c) than the control sample. The SiO_2 from FA, which had not reacted to form hydration product (C-S-H) at this hydration period might have contributed to the increased intensity of Si-O asymmetric stretching band revealing a delayed in pozzolanic reaction for the C30FA and C50FA samples (Figure 9b, c). The higher the FA content, the greater the intensity of Si-O asymmetric stretching band observed. This is in agreement with the XRD result where a higher content of quartz was observed in samples containing 50% FA, than samples with 30% FA at this hydration period (Figure 2c, j, k, l). The peak of υ_3 vibration of the SO_4^{2-} group has been obscured in C30FA and C50FA samples (Figure 9b, c).

An upcoming peak at 3645 cm^{-1} of OH-stretch from $Ca(OH)_2$, which has not being combined in pozzolanic reaction, was observed in C30FA sample (Figure 9b).

Sharper intensity of Si-O asymmetric stretching band (ν_3) and the shift of the Si–O asymmetric stretching vibration to higher wavenumbers as a result of the polymerisation of the SiO_4^{2-} units during C–S–H formation are revealed in samples containing *β*-CD (Figure 9d, e, f). This is an indication of improved hydration reaction compared to *β*-CD samples hydrated for 24 hours and control sample hydrated for 7 days. Reduced intensity of υ_3 vibration of the SO_4^{2-} group and upcoming O-H stretching band from $Ca(OH)_2$ (Figure 9d, e, f) also confirmed hydration reaction. These results correspond to the XRD results, which showed that at the 7 days hydration period, *β*-CD increased the dissolution of C_3S and C_2S and aided the formation of CH, a product of hydration reaction (Figure 2). The early formation of C-S-H and Portlandite (CH) at the 7 days hydration period for samples containing *β*-CD was also revealed in the SEM results (Figure 5d, e).

The transferred effect of *β*-CD in boosting hydration reaction at this hydration period, is revealed in the FA-*β*-CD composite samples (Figure 9g, h, i, j, k, l) showing sharpness of Si-O asymmetric stretching vibration band (ν_3) compared to the C30FA and C50FA samples. When compared to FA-*β*-CD composite samples hydrated for 24 hours (Figure 8), the shift of the Si–O asymmetric stretching vibration to higher wavenumbers, sharper intensity of Si-O asymmetric stretching vibration band (ν_3) and reduced intensity of υ_3 vibration of the SO_4^{2-} group were observed, revealing an improved hydration reaction.

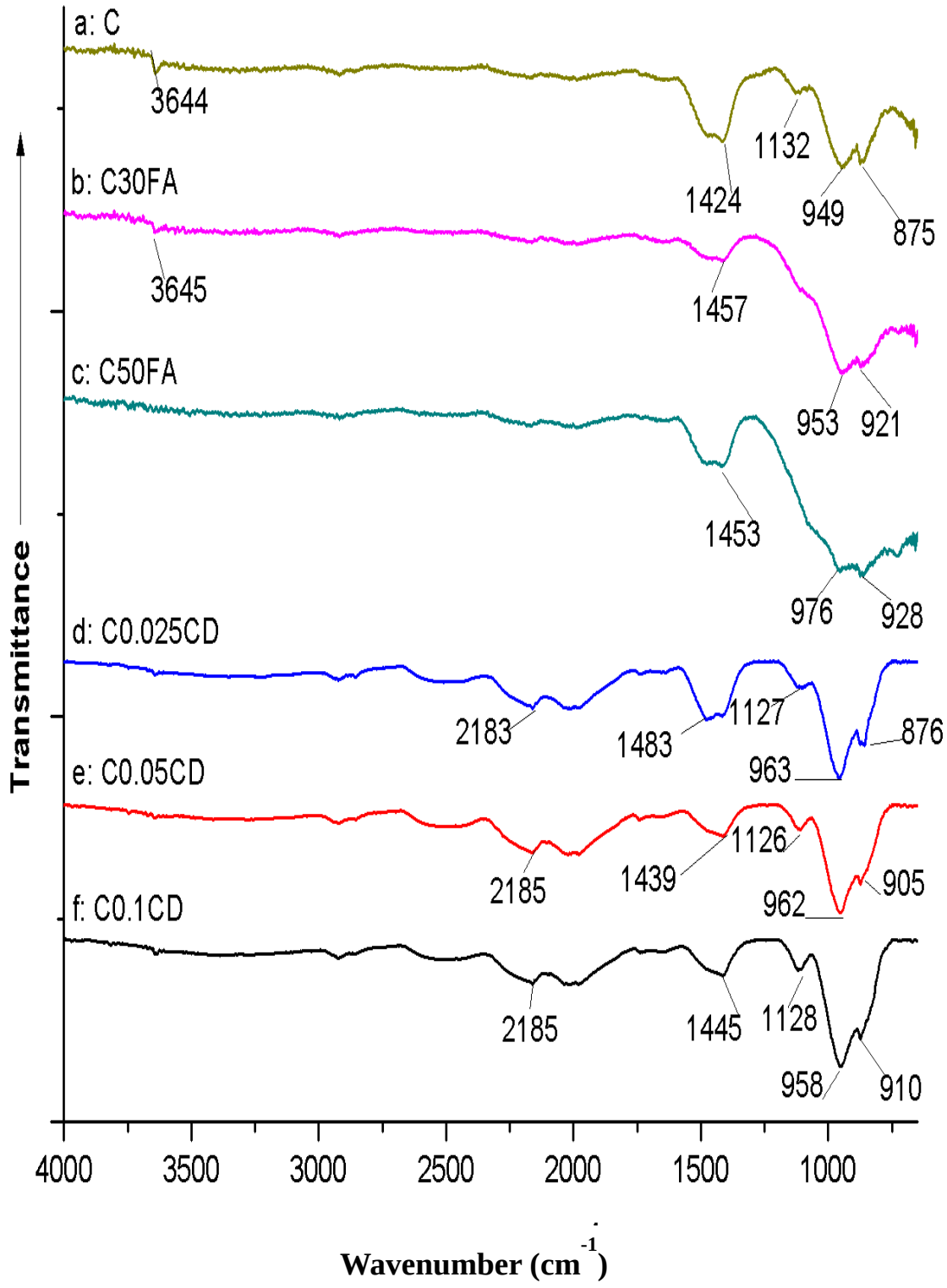

742 *Binary samples (7 days hydration)

743

744

745

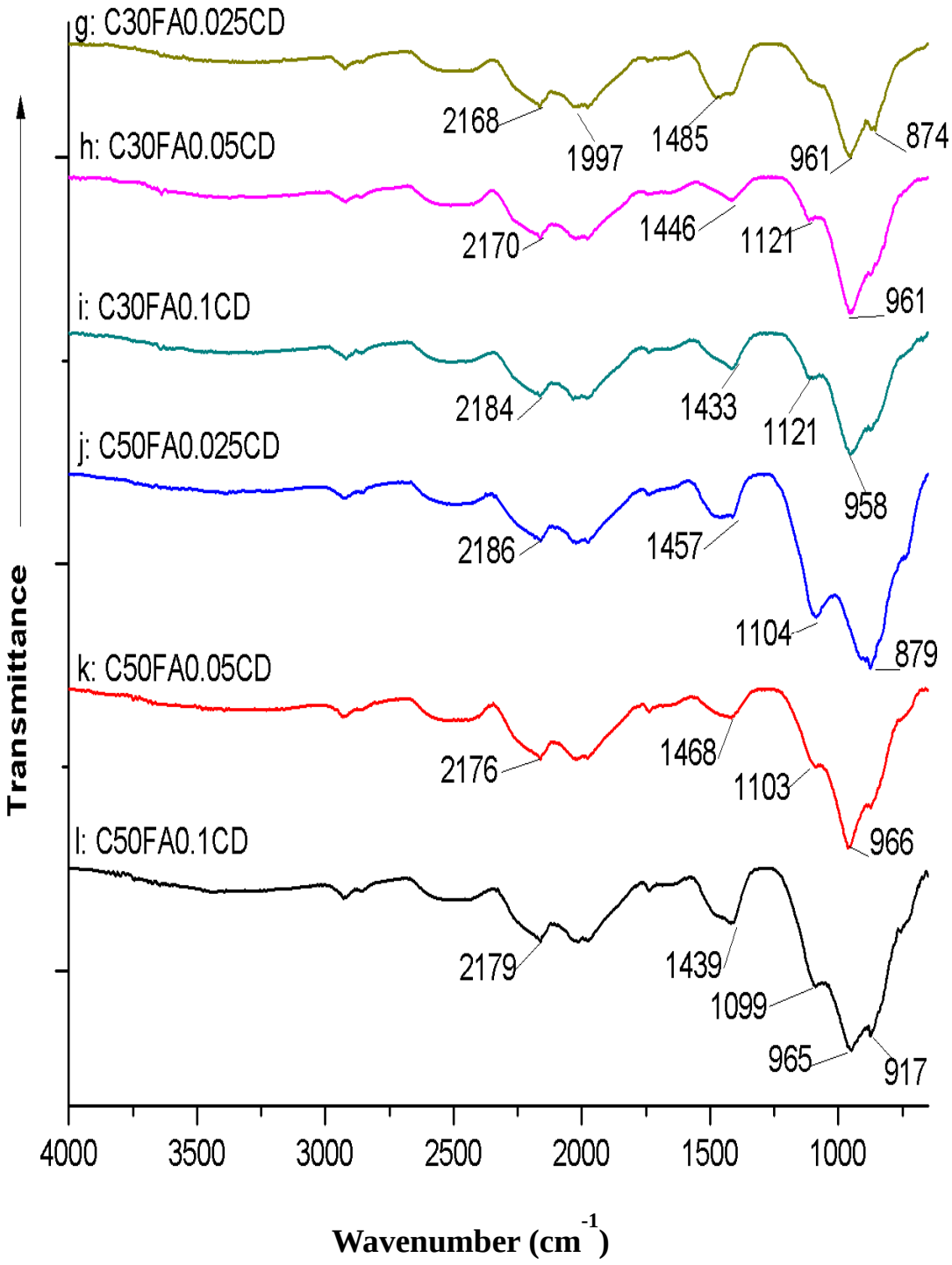

*Ternary samples (7 days hydration)

Figure 9: FT-IR spectra of cement paste of binary and ternary samples hydrated for 7 days

771 **4.3.3 FT-IR analysis after 28 days hydration period**

772 Due to improved hydration and pozzolanic reactions at this hydration age, an increased
773 intensity and sharpness of Si-O asymmetric stretching band was observed for all the samples
774 due to the polymerisation of the SiO_4^{2-} units during C–S–H formation (Figure 10a-l). The
775 sharper intensity of υ_3 vibration of SiO_4^{2-} at the ranges 1435 to 1461 cm^{-1}, showing
776 improved hydration reaction was also observed for all the samples (Figure 10a-l). The
777 reduced intensity of υ_3 vibration of the SO_4^{2-} group at 1126 cm^{-1} of control sample (Figure
778 10a) and shift of Si-O asymmetric stretching band to the higher wavenumber at this hydration
779 period compared to the 7 days hydrated control sample, further showed improved hydration
780 reaction. The reduction in the OH-stretch from $Ca(OH)_2$ at this hydration period compared to
781 7 days might be as a result of $Ca(OH)_2$ being combined with CO_2 in the atmosphere to form
782 more $CaCO_3$ [20, 24]. This is also in agreement with Mollah et al [24] and Bjornstrom et al
783 [26], who reported that the O-H stretching band decreases with the progress of hydration and
784 with the formation of the C–S–H binding phase.

785

786 More defined and sharper Si-O asymmetric stretching bands were observed for C30FA and
787 C50FA samples (Figure 10b, c) at this hydration period than the 7 days hydration period.
788 This is an evidence of improved pozzolanic reaction. The higher the FA content, the greater
789 the intensity observed. There is no sign of an upcoming peak of OH-stretch from $Ca(OH)_2$ for
790 the C30FA and C50FA samples (Figure 10b, c) due to the consumption of $Ca(OH)_2$ during
791 pozzolanic reaction, in addition to other reasons given earlier. This is also in agreement with
792 the XRD results, which revealed a reduction of the CH peak in all the FA samples at the 28
793 days hydration period (Figure 3b, c, g, h, i, j, k, l).

794

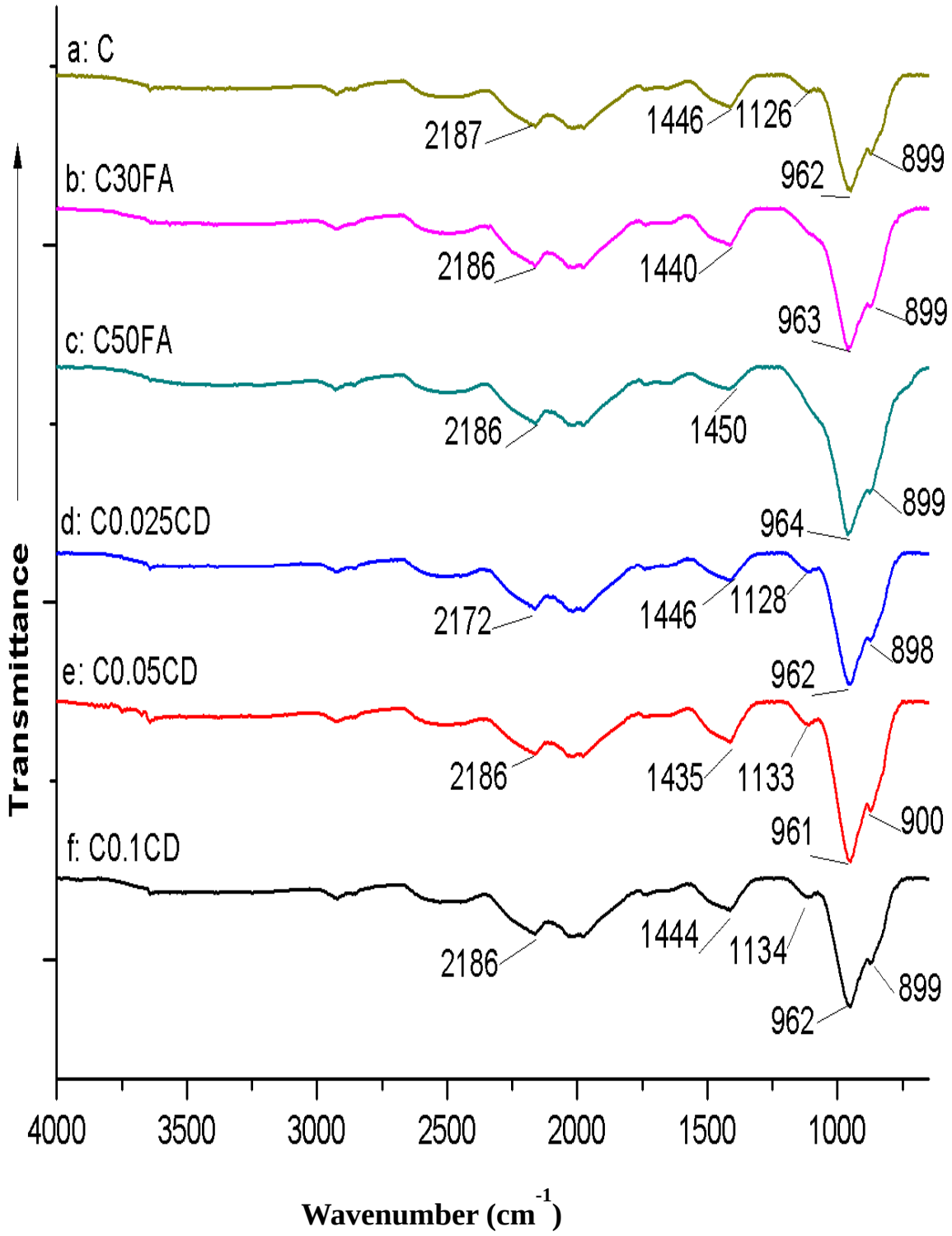

*Binary samples (28 days hydration)

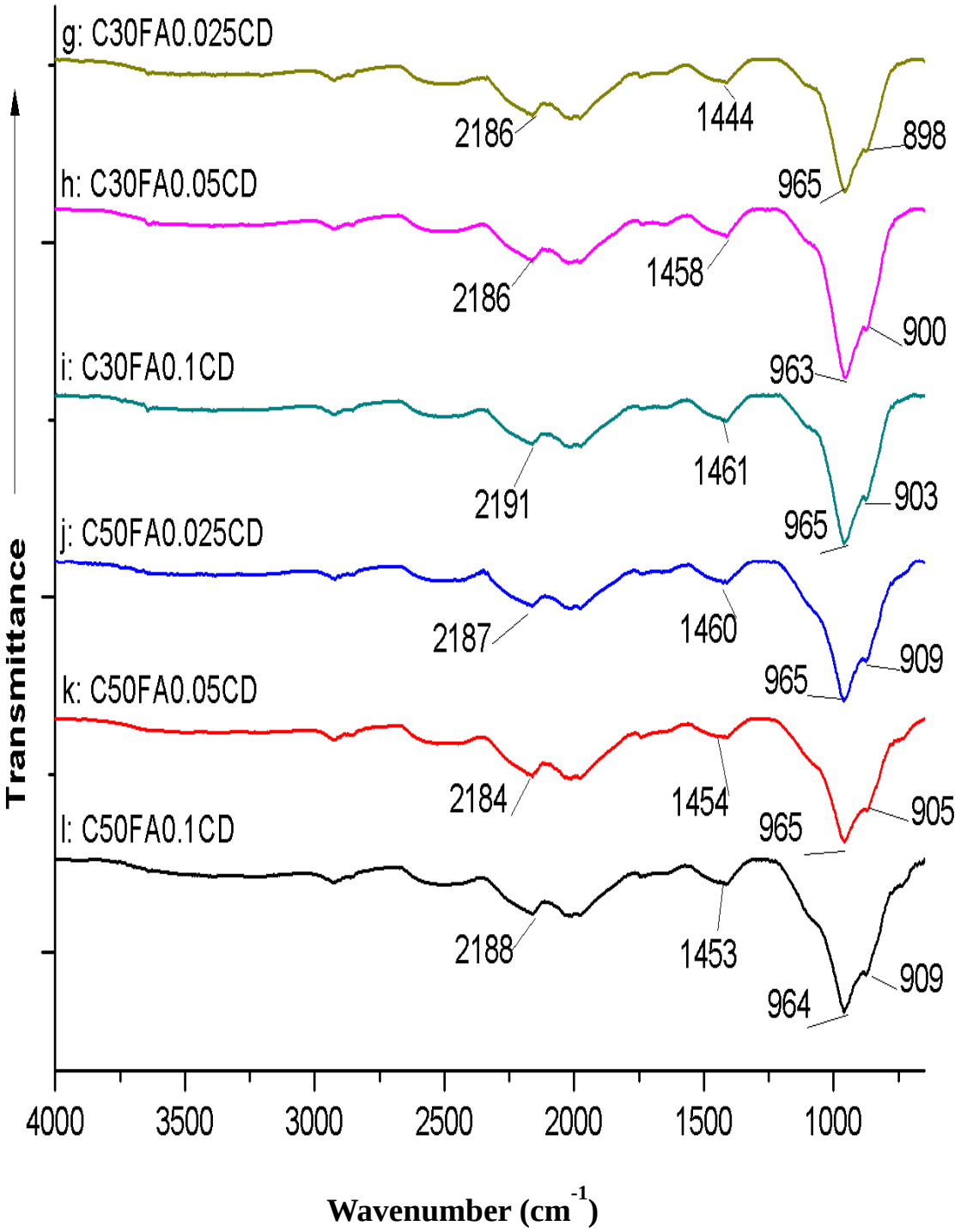

*Ternary samples (28 days hydration)

Figure 10: FT-IR spectra of cement paste of binary and ternary samples hydrated for 28 days

838 **4.3.4 FT-IR analysis after 90 days hydration period**

839 A well advanced hydrated control sample, after a 90 days hydration period, was revealed in
840 Figure 11a. The sharpness of the Si-O asymmetric stretching band and its shift to a higher
841 wavenumber together with a reduced intensity of υ_3 vibration of the SO_4^{2-} group are evidence
842 of an improved hydration reaction of control sample compared to the 28 days hydrated
843 sample. Evidence of an improved pozzolanic reaction was revealed in the C30FA and C50FA
844 samples (Figure 11b, c) through the sharpness of the Si-O asymmetric stretching band and its
845 shift to a higher wavenumber compared to samples hydrated for 28 days. The spectra of the
846 control sample are closely related to the spectra of FA samples, showing that at this hydration
847 period, pozzolanic reaction has caught up with hydration reaction.
848
849 Improved hydration reaction was observed in the *β*-CD samples (Figure 11d, e, f) compared
850 to the 28 days hydrated *β*-CD samples, revealing greater sharpness of the Si-O asymmetric
851 stretching band, shift of the Si-O asymmetric stretching band to higher wavenumber and
852 reduced intensity of υ_3 vibration of the SO_4^{2-}. Greater sharpness of the Si-O asymmetric
853 stretching band was observed for the samples containing 0.025% and 0.1% *β*-CD
854 replacements (Figure 11d, f) compared to control sample. More $Ca(OH)_2$ was formed in the
855 control (Figure 11a) and *β*-CD samples (Figure 11d, e, f) at approximately 3650 cm^{-1},
856 showing an upcoming OH-stretch peak, as also revealed in the XRD results (Figure 4a, d, e,
857 f). The OH-stretch peak from $Ca(OH)_2$ was consumed in all FA (Figure 11b, c) and FA-*β*-CD
858 composites (Figure 11g, h, i, j, k, l) samples due to pozzolanic reaction. A major distinction
859 cannot be traced in the spectra of the FA and the FA-*β*-CD composites samples. The XRD
860 results revealed improved hydration and pozzolanic reactions at 90 days hydration period for
861 samples containing 0.05% and 0.1% *β*-CD replacements (Figure 4 e, f, h, i, k, l).

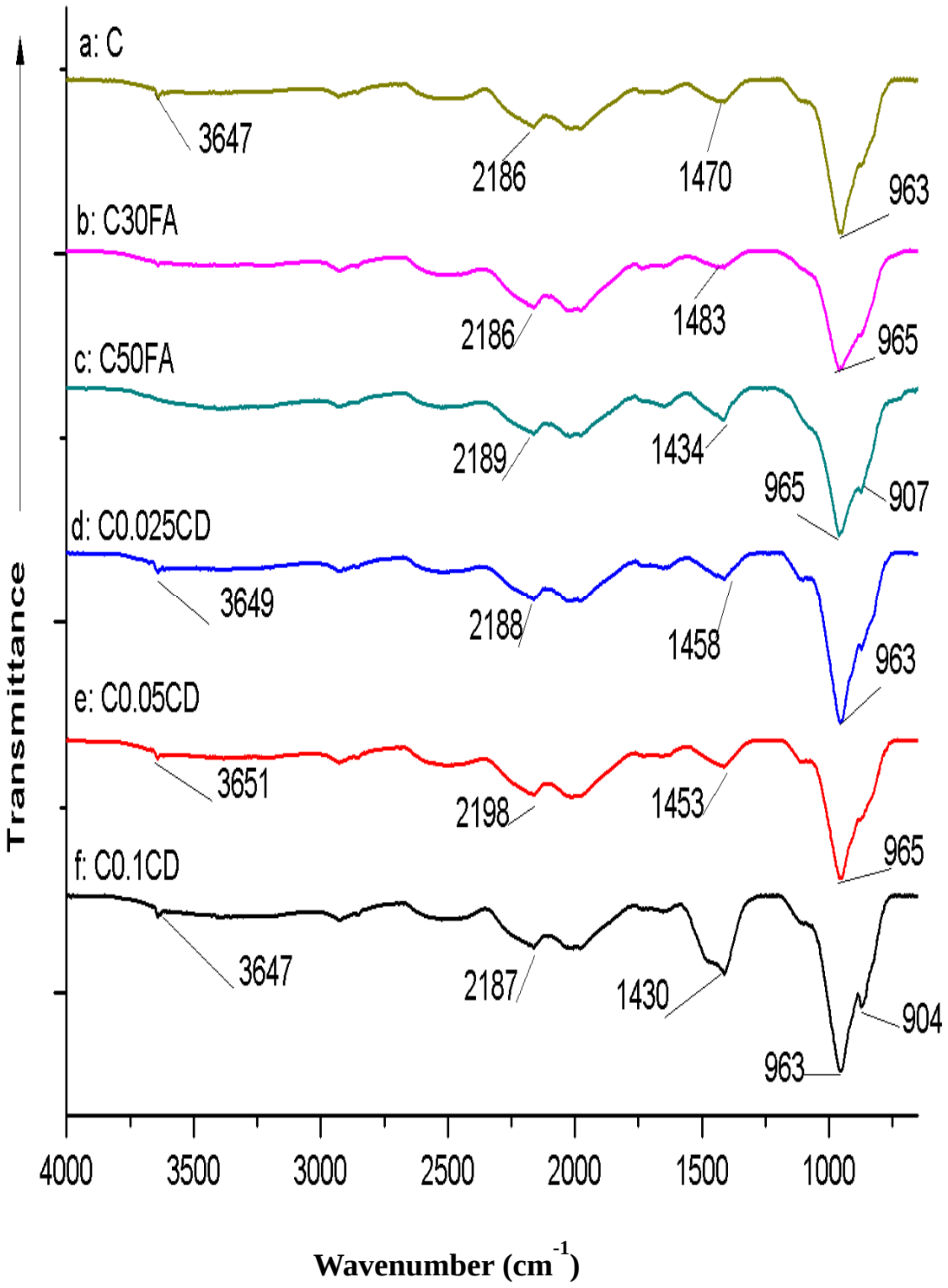

883

884 *Binary samples (90 days hydration)

885

886

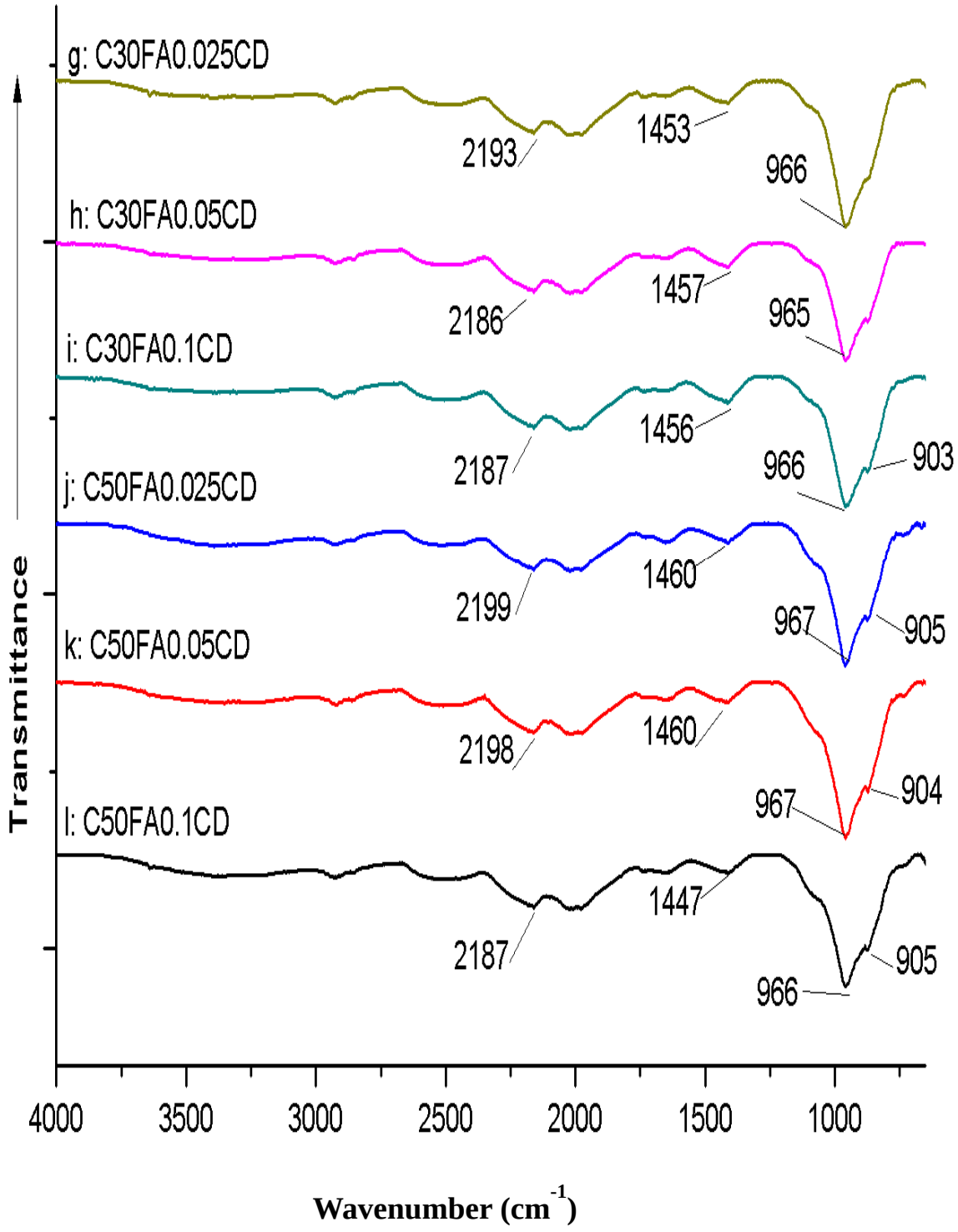

*Ternary samples (90 days hydration)

Figure 11: FT-IR spectra of cement paste of binary and ternary samples hydrated for 90 days

5.0 CONCLUSIONS

The β-CD samples aided both early (from 7 days) and late hydration processes compared to control samples with evidence of increased dissolution of the C_3S and C_2S at the 7 days hydration period and higher formation of CH at the 90 days hydration period. The effect of β-CD on pozzolanic reaction was revealed from the 28 days hydration period in the XRD results.

The morphology of the β-CD samples studied by SEM revealed the crystalline structure of Portlandite (CH) at the 7 days hydration period for the C0.025CD sample compared to the control sample. The higher the β-CD content, the more the dissolution of anhydrous phase of the cement paste was observed in the SEM morphology at 7 days hydration period; as was also confirmed by the XRD results. At the 90 days hydration period, the β-CD and FA-β-CD composite samples showed an improved denser surface and reduced continuous capillary pores compared to the control, C30FA and C50FA samples. The FT-IR results showed that β-CD aided the dissolution of C_3S clinker phase resulting in the greater and sharper intensity of the Si-O asymmetric stretching band (ν_3) of samples containing β-CD compared to control sample at the 24 hour and 7 days hydration periods. At 90 days, the FT-IR spectra of control, FA, β-CD and FA-β-CD composites samples were closely related, revealing that at this hydration period, pozzolanic reaction has caught up with hydration reaction.

6. 0 Acknowledgements

We thank the support of the University of Johannesburg, South Africa and University of South Africa, for making this research possible.

7.0 REFERENCES

[1] Diamond S.: The microstructure of cement paste and concrete a visual primer. Cem and Concr Compos 2004;(26):919–933.

[2] Damme H.V., Gmira A. : Chapter 13.3 Cement hydrates, Handbook of Clay Science Edited by F. Bergaya, B.K.G. Theng and G. Lagaly Developments in Clay Science, Vol. 1, Elsevier Limited, 2006;1113- 1127.

[3] Girão A.V., Richardson I.G., Porteneuve C.B., Brydson R.M.D.: Composition, morphology and nanostructure of C–S–H in white Portland cement pastes hydrated at 55 °C. Cem and Concr Res 2007;(37):1571–1582.

[4] Moir G.: Cement, Advanced Concrete Technology Set, 3–45 (2003).

[5] Aimin X., Sarkar S.L: Microstructural study of gypsum activated fly ash hydration in cement paste. Cem and Concr Res 1991;1137-1147.

[6] Ikotun B.D., Mishra S., Fanourakis G.C.: Study on the synthesis, morphology and structural analysis of fly ash–cyclodextrin composite. J of Incl Phenom and Macro Chem 2014; (79):311-317.

[7] Hughes T.L., Methven C.M., Jones T.G.J., Pelham S.E., Fletcher P., Hall C.: Determining Cement Composition by Fourier Transform Infrared Spectoscopy. Adv Cem Bas Mat 1995;(2),91-104.

955 [8] Ikotun B. D., Fanourakis G. C., Mishra S.: Indicative tests on the effect of fly ash - β
956 cyclodextrin composite on concrete workability and strength. Publication in the RILEM
957 proceedings PRO 95 for the International RILEM Conference on Application of
958 superabsorbent polymers and other new admixtures in concrete construction, at Germany
959 from 14 September 2014 to 17 September 2014. ISBN 978-2-35158-147-6, pages 55 –
960 64.
961
962 [9] Ikotun B. D**.,** Fanourakis G. C., Mishra S.: Indicative tests on the effect of fly ash - β
963 cyclodextrin composite on mortar and concrete permeability, sorptivity and porosity.
964 Publication in the proceedings of the first International Conference on Construction
965 Materials and Structures, from 24 November to 26 November 2014, Johannesburg, South
966 Africa. ISBN 978-1-61499-465-7, pages 825 – 834.
967
968 [10] SANS 5861-3: 2006: South African national standard. Concrete tests, Part 3: Making
969 and curing of test specimens, ISBN 978-0-626-27130-5. Edition 2.1.
970
971 [11] Jain N.: Effect of nonpozzolanic and pozzolanic mineral admixtures on the hydration
972 character of ordinary Portland cement. Constr and Building Mat 2012;(27): 39–44.
973
974 [12] Ali A.H., Kandeel A. M., Ouda A. S.: Hydration Characteristics of Limestone Filled
975 Cement Pastes. Chem and Mat Res 2013;(5):68-73.
976
977 [13] Burgos-Montes O., Alonso M.M., Puertas F.: Viscosity and water demand of limestone-
978 and fly ash-blended cement pastes in the presence of superplasticisers. Constr and
979 Building Mat 2013;(48):417–423.

980 [14] Deschner F., Lothenbach B., Winnefeld F., Neubauer J.: Effect of temperature on the
981 hydration of Portland cement blended with siliceous fly ash, Cem and Concr Res
982 2013;(52):169–181.
983
984 [15] Khater H.M: Effect of silica fume on the characterization of the geopolymer materials.
985 Int J of Adv Struc Eng 2013; 5(12):2-10.
986
987 [16] Pandya S.J., Mansuri J.S., Patel P.: Compatible Polymer used as complexes in various
988 drug delivery systems : β-Cyclodextrin. Pharm Rev 2008;6(2).
989
990 [17] Roncero J., Valls S., Gettu R.: Study of the influence of superplasticizers on the
991 hydration of cement paste using nuclear magnetic resonance and X-ray diffraction
992 techniques. Cem and Concr Res 2002;(32):103–108.
993
994 [18] Snellings R., Salze A., Scrivener K.L.: Use of X-ray diffraction to quantify amorphous
995 supplementary cementitious materials in anhydrous and hydrated blended cements. Cem
996 and Concr Res 2014;(64):89–98.
997
998 [19] Tang S.W., Li Z.J., Shao H.Y., Chen E.: Characterization of early-age hydration process
999 of cement pastes based on impedance measurement Constr and Building Mat 2014;(68):
1000 491–500.
1001
1002 [20] Mollah Y.A., Hess T.R., Tsai Y., Cocke D.L.: An FT-IR and XPS Investigations of the
1003 effects of carbonation on the solidification/stabilization of cement based systems-Portland
1004 type V with zinc. Cem and concr res 1993;(23):773-784.

1005 [21] Omotoso O.E., Ivey D.G., Mikula R.: Characterization of chromium doped tricalcium
1006 silicate using SEM/EDS, XRD and FT-IR. J of Hazardous Mat 1995;(42): 87-102.
1007
1008 [22] Mollah M.Y.A, Lu F., Cocke D.L.: An X-ray diffraction (XRD) and Fourier transform
1009 infrared spectroscopic (FT-IR) characterization of the speciation of arsenic (V) in
1010 Portland cement type-V. The Sci of the Total Env 1998;(224):57-68.
1011
1012 [23] Ylmén R., Jäglid U., Steenari B., Panas I.: Early hydration and setting of Portland
1013 cement monitored by IR, SEM and Vicat techniques. Cem and Concr Res 2009;(39):433–
1014 439.
1015
1016 [24] Mollah M.Y.A., Yu W., Schennach R., Cocke D.L.: A Fourier transform infrared
1017 spectroscopic investigation of the early hydration of Portland cement and the influence of
1018 sodium lignosulfonate. Cem and Concr Res 2000;(30):267–273.
1019
1020 [25] Zhang Z., Wang H., Provis J.L.: Quantitative study of the reactivity of fly ash in
1021 geopolymerization by FT-IR. J of Sust Cem-Bas Mat 2012;1(4):154–166.
1022
1023 [26] Bjornstrom J., Martinelli A., Matic A., Borjesson L., Panas I.: Accelerating effects of
1024 colloidal nano-silica for beneficial calcium–silicate–hydrate formation in cement. Chem
1025 Phy Letters 2004;(392):242–248.
1026
1027 [27] Knapen E., Gemert D. V.: Cement hydration and microstructure formation in the
1028 presence of water-soluble polymers. Cem and Concr Res 2009;(39):6–13.
1029